

STRUCTURE AND DYNAMICS OF MODULATED TRAVELING WAVES IN CELLULAR FLAMES

A. Bayliss, B. J. Matkowsky and H. Riecke
*Department of Engineering Sciences and Applied Mathematics
Northwestern University, Evanston, IL 60208*

ABSTRACT. We describe the formation and evolution of spatial and temporal patterns in cylindrical premixed flames. We consider the cellular regime, $Le < 1$, where the Lewis number Le is the ratio of thermal to mass diffusivity of a deficient component of the combustible mixture. A transition from stationary, axisymmetric flames to stationary cellular flames is predicted analytically if Le is decreased below a critical value. We present the results of numerical computations to show that as Le is further decreased, with all other parameters fixed, traveling waves (TWs) along the flame front arise via an infinite-period bifurcation which breaks the reflection symmetry of the cellular array. Upon further decreasing Le we find the development of different kinds of periodically modulated traveling waves (MTWs) as well as a branch of quasiperiodically modulated traveling waves (QPMTWs). These transitions are accompanied by the development of different spatial and temporal symmetries including period doublings and period halvings in appropriate coordinate systems. We also observe the apparently chaotic temporal behavior of a disordered cellular pattern involving creation and annihilation of cells. We analytically describe the stability of the TW solution near its onset using suitable phase-amplitude equations. Within this framework one of the MTW's can be identified as a localized wave traveling through an underlying stationary, spatially periodic structure.

1. INTRODUCTION. It has been long known that premixed gaseous combustible mixtures do not necessarily burn in a uniform manner. In particular, under certain conditions flame fronts can exhibit a cellular structure, characterized by periodic arrays of crests along the flame front pointing in the direction of the combustion products. The pointed crests are connected by smooth troughs that are convex toward the fresh fuel mixture. The temperature is higher at the troughs, which therefore appear brighter, and lower at the crests, which therefore appear darker [38]. In many instances the transition from laminar to turbulent combustion occurs as a smooth flame breaks up into cells, which then undergo transitions leading to increasingly complex spatial and temporal behavior.

In [38] both stationary and propagating cellular flames were observed on a slot burner, leading to a linear array of cells, while rotating cellular flames were observed on a burner of circular cross section. A variety of cellular patterns have been observed for flames stabilized on a circular burner. In [28] various patterns of ordered cellular flames were observed. For some of the patterns the cells appeared to be essentially stationary, although there was a very small background fluctuation of the intensity, the origin of which was not clear. The cells appeared to be reflection symmetric with respect to both intensity and shape. In [31] both rotating and modulated rotating

cellular states were observed. The rotating cellular flames were characterized by an essentially uniform rotation rate with no visually detectable change in the cellular structure as the cells rotated. The modulated rotating state exhibited a modulation in cell size, intensity and angular velocity. In both cases the cells appeared to be asymmetric in intensity and shape, i.e., the reflection symmetry was broken.

In [29] a different type of dynamical state was observed, in which one or more members of a cellular array underwent a rapid motion while the other members of the array were nearly stationary. In these states, termed hopping states, the hopping cells were noticeably asymmetric while the nearly stationary cells appear to be nearly symmetric. We note that this type of mode was observed earlier where it was termed a square dance mode [25].

In addition to laminar dynamical behavior, chaotic behavior has also been observed. In [30] four different manifestations of chaotic cellular flames are characterized. In particular disordered states are observed, characterized by erratic spatial and temporal behavior, exhibiting creation and annihilation of cells as well as a chaotic variation in intensity, location and cell size. Similar behavior has been observed in [38].

One scenario for the development of cellular flames and the subsequent development of complex spatiotemporal behavior is that of thermo-diffusive cellular instabilities [37, 41, 51], which are obtained from the diffusional thermal model [42] in which the thermal expansion of the gas is assumed to be weak. The model accounts for transport and reaction of heat and one or more components of the combustible mixture, as well as advection due to the flow field, which is specified in advance from a nonreacting flow calculation. Many of the characteristics of observed cellular flames, including complex spatiotemporal flame patterns, can be qualitatively described as thermo-diffusive instabilities. Analytical methods have been successful in describing primary transitions to cellular flames (e.g. [27, 37, 41, 44]). In some cases higher order transitions can be found by analytical methods as well [43, 44]. In most instances, however, secondary and higher order transitions are difficult to find analytically and are more readily found by numerically continuing the analytically predicted solution branches until transitions are found and then following the new branches.

In this paper we consider cylindrical flames, in particular adiabatic flames stabilized by a line source of fuel of strength $2\pi\kappa$. We assume no axial variation and restrict attention to an axial cross section. Thus we solve the problem for a fixed axial slice and employ polar coordinates within this cross section. We further assume that there is a deficient component of the combustible mixture, so that when this component is depleted no further reaction occurs. The model then reduces to two coupled reaction diffusion advection equations. It is characteristic of combustion problems that the activation energies are large. As a result the reaction terms are important only in a thin layer called the reaction zone. In the limit of infinite activation energy the reaction zone shrinks to a surface called the flame front across which certain jump conditions hold. While we consider the finite activation energy case, for which,

strictly speaking, there is no front, we will use this terminology when appropriate. Away from the reaction zone the variables change more gradually. The cellular patterns are most pronounced in the narrow reaction zone, where the dynamics are very sensitive to the accuracy of the computation.

The computations build upon and extend analytical and numerical results previously obtained for this problem. We first describe the analytical results. There are two parameters for this system, κ and the Lewis number, Le , the ratio of thermal to mass diffusivity. In the infinite activation energy limit this system admits, for all values of κ and Le , a stationary axisymmetric solution describing a circular flame front [27, 41]. This solution, called the basic solution, is subject to two different classes of instabilities depending on whether Le is greater than or less than 1.

There exists a critical value, $Le_{c1} > 1$, such that for $Le > Le_{c1} > 1$, the basic solution is unstable. The instability arises as two complex conjugate eigenvalues pass into the right half plane, thus suggesting that small disturbances evolve to nonstationary flames, such as axisymmetric pulsating flames, or flames with traveling or standing waves along the flame front. Similar behavior has also been found in other geometries, e.g. [37, 39, 40, 45]. The regime Le sufficiently greater than 1, describing, e.g., lean, heavy hydrocarbon/air mixtures, is often referred to as the pulsating regime.

Below a second critical value $Le_{c2} < 1$ there exists a κ_c such that for $\kappa > \kappa_c$ the basic solution is also unstable. This instability occurs by a pair of real eigenvalues crossing into the right half plane, and small perturbations evolve to stationary cellular flames [27, 41]. This behavior has also been found in other geometries [35, 37, 43, 51]. The regime Le sufficiently smaller than 1, describing mixtures where the deficient component is highly diffusive, for example lean hydrogen/air mixtures or rich, heavy hydrocarbon/air mixtures, is referred to as the cellular regime.

In this paper we consider the cellular regime, $Le < 1$. The analysis in [27, 41] describes the onset of cellular flames as a diffusional thermal instability. However the analysis does not describe the subsequent evolution of these cellular flames into more complex spatial and temporal patterns and in particular the transition to dynamic behavior observed in experiments. These patterns and transitions will be described in this paper by numerically continuing the stationary cellular solution branch found in [27] until new branches are found. We then follow these new branches to describe more complex spatiotemporal behavior.

The analysis in [27, 41]) identified the roles of the two fundamental parameters in promoting diffusional thermal instabilities of cylindrical flames. For the cellular regime, $Le < 1$, the stationary circular flame front can be destabilized by either increasing κ or decreasing Le . In this paper we consider the behavior as Le is decreased for a fixed value of κ . The behavior of the cellular states as κ is increased, with Le fixed, is described in [12].

We first describe previous results on cellular solution branches as Le is reduced. In [11] the behavior of stationary cellular flames was considered. It was shown that reducing Le led to a progressive deepening of the cells and more pronounced crests.

Only stationary solutions were found for the parameter values used in the computation. In [6] we considered lower values of Le , and found nonstationary 4 cell solutions arising via a secondary transition, i.e., a transition from the branch of stationary 4 cell flames (S4 branch). These solutions described slowly rotating cellular flames. The rotation occurred at a constant angular velocity and corresponded to a slowly traveling wave (TW) along the flame front. It was shown [9] that the transition from stationary to rotating behavior occurred as an infinite period, symmetry (parity) breaking bifurcation, in which the reflection symmetry of the cells was destroyed. That is, while each of the stationary cells was reflection symmetric about its centerline, this symmetry was no longer maintained for the TW solutions. We refer to this branch as the TW4 branch and will describe it in more detail below.

The TW4 branch was a pure 4 cell branch, that is, each solution on this branch was $2\pi/4$ periodic in the angular variable ψ . Stable mixed mode solution branches were also found and described in [9]. The spatial behavior of these mixed mode solutions was that of a 4 cell array in which at any fixed instant of time the cells differed in size (e.g., distance between successive minima of the temperature field) and shape. At any fixed spatial location the temperature and concentration for these mixed mode cellular flames were quasiperiodic in time. Two branches of mixed mode solutions were identified. The first branch appeared to be stable over a small window in Le near the point where the TW4 branch bifurcates from the S4 branch. The second branch was found for values of Le smaller than those for which stable TW4 solutions could be found.

In [14] we presented preliminary results identifying the quasiperiodic mixed mode flames as MTWs, in which, after a certain time interval the solution recovers its structure along the front except for a phase shift [18]. Thus the solution becomes periodic when viewed in an appropriately chosen rotating coordinate system. In this paper we extend the results in [14], identifying additional MTW branches as well as a new MTW-like branch in which the cells are quasiperiodically rather than periodically modulated.

We note that in our computations the periodic direction is the polar angle ψ . Thus the period for physically relevant solutions is fixed (2π) and is not a parameter to be varied as in other problems. Consequently the number of cells associated with the MTWs, as well as the stability of the various solution branches, is determined by parameters related to the gaseous mixture (e.g., κ and Le) rather than by an assumed period of the solution. For the parameters considered here, the MTW and MTW-like branches involve 4 cells rotating about the cylindrical axis. While results are presented here for a fixed value of κ , we believe that similar results, possibly involving a different number of cells, would occur for other values of κ . There are complex cellular structures and symmetries associated with each of the branches in addition to the modulation dynamics. The cellular structures, including symmetries, as well as the dynamics will be described in detail here. We also point out the relationship of the calculated MTW solutions to experimentally observed flames [29, 31]. While

our results are for a simplified model of combustion, the striking similarities between the computed modes and those observed in experiments indicates that the cellular dynamics predicted here does indeed describe those occurring in real flames.

Specifically, we identify three distinct MTW branches, each differing from the others in the nature of the modulation and the symmetries associated with the modulation of successive cells. These are referred to as the PMPY (Pushmi-Pullyu) branch, the BMTW (breathing MTW) branch and the HPMTW (half-period MTW) branch, each of which is described below. In addition, we identify a quasiperiodically modulated traveling wave (QPMTW) mode, characterized by a quasiperiodic modulation involving two apparently independent frequencies. Since there is a third frequency associated with the rotation rate, this mode has three apparently incommensurate frequencies thus describing a 3-torus.

We now briefly describe the nature of the solutions on each of the MTW branches. Solutions along each branch are composed of 4 cells, which exhibit varied dynamical behavior. Solutions along the PMPY branch exhibit a modulation which is strikingly different from the other modulations that we observe. Along the PMPY branch the solution at any instant of time is composed both of nearly stationary, nearly reflection symmetric cells and of nonstationary, asymmetric cells. Motion of the individual cell proceeds as a localized wave of asymmetry travels through the underlying stationary, symmetric cellular array. This behavior is analogous to the hopping modes observed experimentally in [29] and also in [25] where it was termed the “square dance mode”. Along the other two MTW branches the rotation rate about the cylindrical axis is a periodic (nearly sinusoidal) modulation of the uniform rate characteristic of the traveling wave (TW4) branch. The cells also undergo a periodic (nearly sinusoidal) expansion and contraction in both size and intensity (maximum temperature within the cell). In a frame moving with the uniform rotation rate the cells would appear to undergo a breathing motion. The solution is characterized by the symmetry that the modulation is the same for each cell, modulo a constant (in time) phase difference between any two cells. For one of the branches there is no other apparent symmetry. In view of the breathing motion we refer to this branch as the BMTW branch (breathing modulated traveling wave). On the other solution branch alternate cells undergo a modulation with no phase difference between them, so that the solution is periodic over the interval $0 \leq \psi \leq \pi$. Since the angular period has been halved, relative to the BMTW branch, we refer to this branch as the half-period modulated traveling wave (HPMTW) branch. Finally, the QPMTW branch differs from the MTW branches in that the modulation is quasiperiodic rather than periodic and the motion appears to be characterized by three independent frequencies. The solution exhibits the symmetry that alternate cells undergo the same modulation with a constant phase difference between them. Adjacent cells undergo distinctly different modulations. As Le is decreased further the QPMTW branch as well as the HPMTW branch appear to lose stability to an attractor which seems to exhibit chaotic temporal behavior along with a disordered spatial pattern involving cells undergoing an erratic motion

and creation and annihilation of cells in an apparently random fashion. This behavior is characteristic of weakly turbulent flames.

MTWs have been found previously in other parameter regimes in combustion as well as in other physical systems. In [10] MTWs were found for nonadiabatic cellular flames in the pulsating regime. These modes were shown to be stages in the development of chaotic behavior for flames near extinction. MTWs have been computed for the Kuramoto-Sivashinsky equation describing combustion and other areas of application [18], and have also been observed in non-reacting flows e.g., in Taylor-Couette flow experimentally [32], and computationally [21].

The accuracy of the computed solution is very sensitive to the resolution of the reaction zone, the location of which is not known beforehand. As a result, adaptive procedures are needed to locate and resolve the reaction zone as the solution evolves in time. The problem of obtaining adequate resolution of the reaction zone is further complicated by the extremely deep cells which occur as Le is decreased. We employ an adaptive pseudo-spectral method which has been used successfully for a variety of other problems in combustion (see, e.g., [3, 4, 5]). We describe the model in section 2 and the numerical method in Section 3. In Section 4 we describe our results in detail. In section 5 we provide an analytical description of the transition to the TW4 branch within the framework of a resonant mode interaction. In addition, we employ suitable phase-amplitude equations to discuss its stability as well as the transition to the PMPY branch.

2. MATHEMATICAL MODEL. We consider the problem of a flame stabilized by a line source of fuel of strength $2\pi\kappa$. We assume that the reaction is limited by a single deficient component and is governed by one step, irreversible Arrhenius kinetics. We denote dimensional quantities by $\tilde{\cdot}$. The unknowns are the temperature \tilde{T} and the concentration \tilde{C} of the deficient component. \tilde{T}_u and \tilde{T}_b are the temperatures of the unburned and burned fuel respectively and \tilde{C}_u is the unburned value of \tilde{C} . Other dimensional quantities are the coefficient of thermal diffusivity $\tilde{\lambda}$, the activation energy \tilde{E} , and the gas constant \tilde{R} . We introduce the nondimensional reduced temperature and nondimensional concentration by

$$\Theta = (\tilde{T} - \tilde{T}_u)/(\tilde{T}_b - \tilde{T}_u), \quad C = \tilde{C}/\tilde{C}_u.$$

The spatial and temporal variables are nondimensionalized by

$$t = \frac{\tilde{t}\tilde{U}^2}{\tilde{\lambda}}, \quad x_i = \frac{\tilde{x}_i\tilde{U}}{\tilde{\lambda}},$$

where \tilde{U} is the planar adiabatic flame speed for the case of infinite activation energy in which the reaction term is replaced by a surface delta function. We employ polar coordinates (r, ψ) , and the nondimensionalized flow velocity due to the fuel source is

$\mathbf{V} = \frac{\kappa}{r} \hat{\mathbf{r}}$ where $\hat{\mathbf{r}}$ is the unit radial vector. The equations of the diffusional thermal model are [41]

$$\begin{aligned}\Theta_t &= \Delta\Theta - \frac{\kappa\Theta_r}{r} + C\Lambda \exp\left(\frac{Z(\Theta - 1)}{\sigma + (1 - \sigma)\Theta}\right), \\ C_t &= \frac{\Delta C}{Le} - \frac{\kappa C_r}{r} - C\Lambda \exp\left(\frac{Z(\Theta - 1)}{\sigma + (1 - \sigma)\Theta}\right).\end{aligned}\tag{1}$$

Here Δ is the Laplacian, $\sigma = \tilde{T}_u/\tilde{T}_b$, $N = \tilde{E}/(\tilde{R}\tilde{T}_b)$, Le is the Lewis number, and $\Lambda = Z^2/(2Le)$, where $Z = N(1 - \sigma)$ is the Zeldovich number. We note that Λ , which is referred to as the flame speed eigenvalue, depends on the nondimensionalization. The value employed above arises from the use of the planar, adiabatic flame velocity in the infinite activation energy limit $Z \rightarrow \infty$. A different nondimensionalization would change the spatial and temporal scales but would not alter the basic patterns exhibited by the solution. The boundary conditions are

$$\begin{aligned}C &\rightarrow 1, & \Theta &\rightarrow 0 \text{ as } r \rightarrow 0, \\ C &\rightarrow 0, & \Theta &\rightarrow 1 \text{ as } r \rightarrow \infty.\end{aligned}\tag{2}$$

In our computations these boundary conditions are imposed at points r_1 and r_2 far from the reaction zone where combustion occurs. The computed results were found to be insensitive to changes in r_1 and r_2 .

The solution to (1)-(2) has been studied analytically in the limit $Z \rightarrow \infty$, and $Le - 1 = \rho/Z$ [27, 41]. In this limit the reaction zone shrinks to a surface $r = \Psi(\psi, t)$, called the flame front. The following stationary, axisymmetric solution exists for all values of κ and Le :

$$\begin{aligned}\Theta &= \begin{cases} (r/\kappa)^\kappa + O(1/Z), & r \leq \kappa, \\ 1, & r \geq \kappa, \end{cases} \\ C &= 1 - \Theta + O(1/Z), \\ \Psi &= \kappa,\end{aligned}$$

and is referred to as the basic solution. The dependence of the solution on ρ enters in the $O(1/Z)$ terms, not written explicitly here.

This solution becomes unstable if $Le < Le_c < 1$ and κ is sufficiently large, or if $Le > Le_c > 1$. In the first case a real double eigenvalue (one corresponding to \cos the other to \sin) crosses from the left half plane into the right half plane and a transition from the basic solution to stationary cellular flames occurs [27, 41]. Additional transitions have been obtained numerically and are described in Section 4.

3. NUMERICAL METHOD. We employ an adaptive Chebyshev pseudo-spectral method in r that we previously developed [3, 5], together with a Fourier pseudo-spectral method in ψ . To enhance the resolution of the reaction zone, we adaptively transform r in order to minimize a functional monitoring the numerical error.

We first briefly discuss pseudo-spectral methods. Detailed descriptions of this class of numerical methods can be found in [19, 33]. We transform the domain for the variable r to the interval $(-1, 1)$. Here we denote the transformed variable by r as well. The solution, u , which generically represents either Θ or C , is then expanded as a sum of basis functions

$$u \simeq u_J \equiv \sum_{j=0}^J a_j \phi_j(r). \quad (3)$$

In a Fourier method the basis functions ϕ_j are trigonometric. In a Chebyshev method the basis functions ϕ_j are the Chebyshev polynomials, i.e. $\phi_j(r) = T_j$ where T_j is the j^{th} Chebyshev polynomial,

$$T_j(r) = \cos(j \cos^{-1}(r)).$$

The expansion coefficients a_j are obtained from collocation, that is, the function u_J is forced to solve the equations at a set of $J + 1$ collocation points r_j . We employ the Gauss-Lobatto points,

$$r_j = \cos(j\pi/J), \quad 0 \leq j \leq J,$$

as collocation points. Thus in a pseudo-spectral method the unknowns are the solution values at the collocation points. The expansion (3) is only used to compute spatial derivatives. The Fourier method is similar, except that trigonometric functions are used as basis functions.

The major advantage of pseudo-spectral methods over finite difference methods is enhanced accuracy for a fixed discretization size. In fact pseudo-spectral methods exhibit infinite order accuracy when used to approximate infinitely differentiable functions, that is, the error can be shown to decrease faster than any inverse power of J . These methods are commonly used to approximate problems where a high degree of accuracy is required, for example in the study of fluid dynamical instabilities, (see, e.g., [19]). However, although these methods are highly accurate when used to approximate functions which exhibit relatively gradual spatial variation, they have difficulties in approximating functions exhibiting localized regions of rapid variation, such as the temperature rise and concentration decay across the narrow reaction zone. Severe spatial oscillations can occur in approximating rapidly varying functions which are not well resolved [19, 33]. These oscillations can affect the computed dynamics and in certain cases lead to the computation of spurious dynamics (for example inadequately resolved computations can indicate chaotic behavior whereas the exact solution is in fact periodic).

If the location of the reaction zone were known in advance, the oscillations could be eliminated by introducing a suitable change of coordinates so that in the new coordinate system the solution has a more gradual variation. However, typically the location of the reaction zone is not known in advance and is one of the objects of the computation. In order to realize the benefits (high accuracy) of the pseudo-spectral method in computing solutions which vary rapidly in localized regions of

space, we developed an adaptive pseudo-spectral method. This method has proven to be effective in computing the rapidly varying solutions which occur in combustion problems. The method is described in detail in [3, 5]. The description we give here will be brief.

We introduce a family of coordinate transformations of the form

$$r = q(s, \vec{\alpha}) \quad (4)$$

where s is the new computational coordinate and $\vec{\alpha}$ represents a parameter vector which is typically of low dimension. We choose $\vec{\alpha}$ so that in the new coordinate system the solution exhibits a more gradual variation and thus is better approximated by a small number of basis functions. Since the behavior of the solution changes during the course of the computation, appropriate values of $\vec{\alpha}$ must be chosen adaptively so as to adapt to changes in the solution [3, 5]. The choice of the coordinate transformations, which we discuss below, is motivated by the asymptotic notion of "stretching" a layer in the method of matched asymptotic expansions [16, 34] for treating singular perturbation problems.

In order to adaptively choose a coordinate transformation in which the spectral approximation is more accurate we employ error measures which are computed for each value of $\vec{\alpha}$ until a minimum is found. In this paper the error measure is the functional

$$I_2(g) = \left(\int_{-1}^1 (L^2 g)^2 / w(s) ds \right)^{\frac{1}{2}}, \quad (5)$$

where

$$w(s) = \sqrt{1 - s^2}, \quad L = w(s) \frac{d}{ds}.$$

It can be shown that this functional gives an upper bound on the maximum norm of the error in approximating a function by its Chebyshev expansion [3].

A very important feature of the adaptive pseudo-spectral method is the particular family of mappings. The unknowns Θ and C vary gradually except in and near the reaction zone where rapid changes occur. We employ a family of mappings, introduced in [15], in which functions with properties similar to these are mapped into linear polynomials, which can be approximated using a relatively small value of J .

In order to describe this family of mappings, we let I denote the interval $-1 \leq r \leq 1$ and consider the family of functions

$$h(r, \alpha_1, \alpha_2) = s_0 + \tan^{-1}(\alpha_1(r - \alpha_2)) / \lambda. \quad (6)$$

The parameters s_0 and λ are determined so that (6) maps the interval I univalently onto itself,

$$s_0 = \frac{\beta - 1}{\beta + 1}, \quad \beta = \tan^{-1}(\alpha_1(1 + \alpha_2)) / \tan^{-1}(\alpha_1(1 - \alpha_2)),$$

$$\lambda = \tan^{-1}(\alpha_1(1 - \alpha_2))/(1 - s_0).$$

When α_1 is large (the analog of ϵ small in singular perturbation problems), (6) is nearly discontinuous with a region of rapid variation occurring near $r = \alpha_2$, i.e., there is an internal layer at $r = \alpha_2$. We observe that other functions, e.g., $\tanh(z)$, can be used in place of $\tan^{-1}(z)$.

The inverse of (6),

$$r = q(s, \vec{\alpha}) = \alpha_2 + \tan((s - s_0)\lambda)/\alpha_1, \quad (7)$$

describes a two parameter family of mappings of I which are one to one and onto, with the property that $h(q(s, \alpha_1, \alpha_2), \alpha_1, \alpha_2)$ is a linear function. If α_1 and α_2 are properly chosen the temperature and concentration profiles will be sufficiently similar to (6) that the composite function can be represented by a small number of Chebyshev polynomials. The parameter α_1 is a measure of the rapid rate of change of the function, while α_2 is related to the location of the layer, i.e. the region of rapid variation. In our method these parameters are determined adaptively by minimizing the functional (5). The equations are integrated in time using a first order splitting method described in [9]. The timesteps are kept sufficiently small so that there is no noticeable effect of temporal integration errors.

In the computation of cellular flames, the location of the reaction zone depends on ψ . In this case the optimal values of α_1 and α_2 will also depend on ψ . A two dimensional adaptive pseudo-spectral method which allows for this dependence has been developed and applied to problems in gasless condensed phase combustion in [4]. The resulting coordinate system is nonseparable, thereby requiring additional computation as described in [4]. The problem considered here is posed in a coordinate system in which the Laplacian is separable and it is more efficient to use one dimensional coordinate transformations which maintain separability (i.e. α_1 and α_2 independent of ψ), even at the expense of not using values of α_1 and α_2 which are optimal for any particular value of ψ . We therefore compute the functional (5) for all angular points and minimize the average, rather than minimizing for each value of ψ . We are nevertheless able to obtain a high degree of resolution of the wrinkled reaction zone due to the effectiveness of the family of mappings (7) in concentrating resolution in a fixed region. As a result, after the mapping is applied Θ and C are no longer rapidly varying in any angular direction although the parameters α_1 and α_2 are generally not optimal for any particular direction.

4. NUMERICAL RESULTS. In this section we present the results of our numerical simulations of eqs.(1) at fixed dimensionless activation energy, $N = 20$, fixed temperature ratio of unburned and burned material, $\sigma = 0.615$, and fixed flow rate, $\kappa = 14.8$, while the Lewis number Le is varied. The timesteps were typically $O(10^{-3})$. In all cases 101 Chebyshev collocation points were sufficient to accurately compute

solutions in the radial direction. We generally used 128 collocation points in the angular direction, although in some cases we employed 256. There was virtually no effect in increasing the number of collocation points in either independent variable. In the radial direction the computational domain was taken as $r_1 \leq r \leq r_2$ with $r_1 = 1, r_2 = 41$. We found virtually no effect in changing these values. The computations presented here were obtained at the NCSA and the NERSC.

An overview of the different solution branches is given in fig.1a where we plot the maximum norm of the difference between the computed cellular solution and the (unstable) axisymmetric solution as a function of Le for the different solution branches that we have found. We generally concentrate on determining the nature of the transitions that occur and on the properties of solutions along different solution branches rather than on determining the precise numerical values of the control parameter Le at which the transitions occur. We note that we solve the initial value problem, marching forward in time until a steady state is achieved, so that in general we only compute stable solutions. However unstable solutions can sometimes be computed by modifying the computer program so as to impose certain symmetries in the angular direction. For example, unstable axisymmetric solutions can be computed by allowing no variation in ψ . Unstable 4 mode solutions can be computed by restricting the computation to the interval $0 \leq \psi \leq 2\pi/4$ and imposing periodicity. Unstable reflection symmetric solutions can be computed by restricting to the interval $0 \leq \psi \leq 2\pi/8$ and imposing reflection symmetry. We have not computed unstable solutions which are not stabilized by the imposition of specific symmetries.

In the regime considered here we find 3 branches of stationary solutions, S4, S5 and S8, which have, 4, 5 and 8 cells respectively. The cells associated with solutions along these branches are reflection symmetric. Only the S4 branch bifurcates stably from the basic axisymmetric state; the S5 and S8 branches are unstable at onset. The S5 branch becomes stable, however, for smaller Le . This behavior is not unexpected since in general only the state closest to the minimum of the neutral curve is stable to sideband instabilities at onset, whereas the other states become stable at the Eckhaus stability (stability to sideband disturbances) limit. When decreasing Le the S4 branch continuously merges with the S8 branch, i.e. the first harmonic becomes increasingly stronger whereas the fundamental eventually goes to zero. Thus, the S4 branch bifurcates from the S8 branch in a pitchfork bifurcation. We will not discuss the behavior of solutions that arise when the S5 branch becomes unstable. We also did not follow the S8 branch for values of Le below those indicated in fig. 1a.

Before reaching the S8 branch, the S4 branch becomes unstable to perturbations which break the reflection symmetry (parity-breaking bifurcation) [9]. To calculate solutions on the S4 branch beyond that point we therefore restrict the solutions to be reflection symmetric. At the parity-breaking bifurcation point a branch of traveling 4 cells, TW4, emanates from the S4 branch. These waves are similar to the rotating cells observed in [31] which were also found to be asymmetric while the nonrotating cells were symmetric. In the computations the rotation rate and the degree of asymmetry

[9] go to 0 continuously as the bifurcation point is approached, indicating that this is an infinite period bifurcation. Strikingly, the TW4 solutions appear to be unstable at onset, although the bifurcation corresponds to a supercritical pitchfork bifurcation. Perturbed solutions evolve either to a solution on the S5 branch or, in a small window of Le , to a solution on a MTW branch which we refer to as the “Pushmi-Pullyu” (PMPY) branch, as discussed below. The relevant instability has the character of a sideband instability and can be suppressed by restricting the domain of computation to $0 \leq \psi \leq 2\pi/4$ and imposing periodicity. In the full domain the TW4 solutions eventually become stable for smaller Le ($Le \leq 0.37$). The instability close to onset may explain why the rotation rates of the waves observed in the experiments [31] do not approach 0 continuously as the transition point is approached.

When Le is decreased further, the TW4 solutions become unstable again and a branch of modulated waves arises in what appears to be a supercritical Hopf bifurcation. Due to the visual appearance of a breathing of the cells we call this 2 frequency state a BMTW. For even smaller values of Le two additional, different branches of modulated waves arise; the QPMTW, which arises from the BMTW branch and appears to be a quasiperiodically modulated wave with three frequencies, and the HPMTW branch which bifurcates from the (unstable) TW4 branch. These branches are shown in detail in fig. 1b. In the following we discuss the properties of the modulated waves in detail.

We first consider the PMPY branch. Fig. 2 shows a contour plot of Θ at fixed t for $Le = 0.42$. The contours have been chosen to emphasize contours of Θ corresponding to values near 0.98 where the cellular structure of the solution is most pronounced. Clearly, none of the 4 cells are exactly alike; two of the cells are nearly reflection symmetric, characteristic of the behavior along the branch S4, while two of the cells are not symmetric, characteristic of the behavior along the branch TW4. The dynamics of this solution is shown in fig. 3 where $\Theta(r_*, \psi, t)$ is shown as a function of ψ for increasing values of t . Here and in the following r_* is chosen so that the circle $r = r_*$ is in the reaction zone. As the forward crest (temperature minimum) of a given cell (cell 3 in the figure if we number the cells from the left) is jerked clockwise (to the left in fig. 3), the cell expands, becomes asymmetric and moves clockwise. This, in turn, pulls the cell behind it (cell 4) so that it too expands, becomes asymmetric and moves clockwise. At the same time cell 3 pushes the cell ahead of it, compressing it and causing it to become nearly symmetric and nearly stationary. This process then repeats with cells 1 and 2 etc. in turn and can be viewed as a *localized* wave of asymmetry propagating counter-clockwise through the stationary symmetric cellular array. This dynamics suggest that the solution is best described as a “Pushmi-Pullyu” [36] solution. Its behavior is analogous to that of the hopping modes observed experimentally in [25, 29]. Similar patterns have been observed in directional solidification [26], in directional viscous fingering [47] and in Taylor vortex flow [52].

Alternatively, it can be seen from fig. 3 that the dynamics of the PMPY solution can also be characterized as that of a MTW, since after a discrete time interval τ the

pattern reemerges, though shifted in space,

$$\Theta(\psi - c\tau, t + \tau) = \Theta(\psi, t). \quad (8)$$

Thus, in a coordinate system rotating uniformly with speed c , $\tilde{\psi} = \psi - ct$, the solution would be periodic. In addition, the PMPY solutions possess the more restrictive symmetry

$$\Theta(\tilde{\psi} + 2\pi/4, t + \tau/4) = \Theta(\tilde{\psi}, t), \quad (9)$$

which connects adjacent cells. It implies that all 4 cells perform the same dynamics although shifted in time. In the context of a discrete or cellular k -mode system with periodicity 2π , the symmetry

$$\Theta(\tilde{\psi} + 2\pi/k, t + \tau/k) = \Theta(\tilde{\psi}, t), \quad (10)$$

referred to as ‘‘ponies on a merry-go-round’’ (POM), is often observed [2, 18].

The BMTW solutions exhibit the same symmetry (9) as the PMPY solutions. The form of modulation, however, is different. This is shown in fig. 4 which illustrates the temporal evolution of $\Theta(r_*, \psi, t)$. In order to understand why the TW4 branch does not persist stably for lower values of Le , we note that the general effect of decreasing Le is to increase the size of the cells, where by the size of the cells we refer to the elevated high temperature region between the two successive minima. Decreasing Le corresponds to increasing the diffusivity of the reactant relative to the diffusivity of heat. As a result the reactant diffuses into a region of higher temperature where a higher degree of burning occurs. This in turn generates more heat which then diffuses, thus raising the temperature over a larger region, which effectively increases the size of the cells. For the values of Le considered, the radial location of the reaction zone does not change significantly. Therefore the cells must fit into the circumference $2\pi r_*$. As Le is decreased, progressively larger cells are forced to fit into the fixed circumference. Beyond a certain point a more stable configuration is that illustrated in fig. 4 where some cells have contracted while their neighbors have expanded. Analysis of the spectrum of the computed solutions indicates that the BMTW branch appears to arise due to a sideband instability whereby TW4 solutions are modulated by a mode 1 modulation.

The following dynamical behavior is observed. Similar to the PMPY solutions the cells undergo an overall rotation with a modulation of cell size and intensity. In contrast to the PMPY solutions, the rotation rate never gets close to 0 and all the cells are asymmetric at all times. Thus the asymmetry is global rather than localized as for the PMPY solutions. In order to illustrate the nature of the modulation, we consider the maxima of $\Theta(r_*, \psi, t)$. We find that for each fixed t , Θ attains exactly 4 maxima for $0 \leq \psi < 2\pi$ which we denote by $\hat{\Theta}_i (i = 1, \dots, 4)$. Clearly each such maximum is identified with an individual cell and may be thought of as a measure of the intensity of the cell. We note that we have accounted for the possibility that any particular maximum may well lie between two angular collocation points. We do so

by accumulating all of the maxima for which ψ is fixed over a time interval and then taking the largest of these maxima. In fig. 5a the temporal evolution of $\hat{\Theta}_i$ is plotted for 2 adjacent cells (i.e., $i = 1, 2$). The figure clearly shows both that the modulation is periodic and is essentially the same for the two cells except for a constant phase shift. Similar properties hold for the other two cells as well. In addition, the phase shift is the same between all pairs of adjacent cells. In fig. 5b the angular location of each maximum is shown as a function of t . Clearly, in addition to their breathing motion the cells undergo a periodic oscillation in position and rotation rate.

Breathing type MTW solutions, somewhat analogous to the BMTW solutions found here, have also been found for nonadiabatic, pulsating ($Le > 1$) flames near extinction [10]. These MTWs also appeared to arise via a bifurcation from a TW flame, specifically a 7 cell TW which was simultaneously destabilized by the subharmonic modes 3 and 4. However the MTWs found in [10] exhibited a different symmetry from the POM symmetry (10). They exhibited the symmetry referred to as “jumping ponies on a merry-go-round” (JPOM) [10],

$$\Theta(\tilde{\psi} + l \times 2\pi/k, t + \tau/k) = \Theta(\tilde{\psi}, t). \quad (11)$$

Whereas the POM symmetry relates each cell to the cell adjacent to it, this symmetry relates cells according to the sequence $1, l + 1, 2l + 1, \dots \pmod{k}$, effectively skipping the $l - 1$ cells between successive members of the sequence. Here $k = 7$ corresponds to the total number of cells. Thus, for example, if at a certain time cell 1 attains its maximum temperature then $1/7th$ of a period later in time cell $1 + l$ would attain its maximum. In an experiment a temperature maximum is observed as a spot of maximum brightness. Thus, with $l \neq 1$ the bright spot would be seen as jumping over the $l - 1$ cells between cells 1 and $1 + l$. The POM symmetry is a special case of (11) with $l = 1$. We note that the general symmetry (11) has been discussed in [48] in the context of rotating fluids. In [10] transitions to JPOM MTWs with $l = 2$, with $l = 4$ and with $l = 1$ (corresponding to the POM symmetry (10)) were found. Thus MTWs exist in two different parameter regimes within the same model of combustion, however the mechanism of instability as well as the symmetries of the resulting MTW, is different in the two cases. In both cases there are additional transitions leading to chaos, but the nature of the transitions is different for the two regimes.

When Le is reduced to about $Le = 0.21$ the BMTW branch becomes unstable and a transition to the QPMTW branch occurs, as the symmetry (9) is broken. Near the transition point the symmetry breaking is most pronounced in the phase differences between pairs of adjacent cells. This is shown in fig. 6a where we plot $\Theta(r_*, \psi, t)$ for $Le=0.205$. It can be clearly seen that cells 1 and 2 (numbered from the left) have a small phase difference between them (in fact they appear to be nearly in phase). Cells 3 and 4 behave similarly. In contrast, the phase difference between cells 2 and 3 and between cells 4 and 1 is considerably larger. As Le is further reduced from the transition point, the differences in the amplitude of the modulation between the odd and even cells becomes more pronounced. This can be seen in fig. 6b where we

plot $\Theta(r_*, \psi, t)$ for $Le=0.180$. In addition, each cell undergoes a modulation in size, similar to the dynamics of the BMTW solutions. However, adjacent cells now undergo different modulations and the 4 cell array splits into two pairs. Within each pair the modulations are nearly in phase while there is a large phase difference between the two pairs. This behavior has the character of a spatial period doubling. We remark that in order to facilitate a comparison between the BMTW, QPMTW and HPMTW branches, both the total temporal duration and the time difference between successive curves, is the same for figs. 6a and 6b as well as for the analogous figs. 4 and 8.

While figs. 6a and 6b give the visual appearance of a periodic modulation, upon closer examination we find that the amplitude of the modulation is quasiperiodic and thus the waves are quasiperiodically modulated. This can be seen in figs. 7 where we examine the temporal evolution of the maxima $\hat{\Theta}_i$. In figs.7a,b the evolution of adjacent and alternate maxima, respectively, is illustrated. For each cell the amplitude modulation is quasiperiodic, with a high frequency oscillation modulated by a low frequency envelope. Alternate cells have the same envelope, and their modulations differ only by a constant phase shift with respect to the envelope. Adjacent cells have distinctly different envelopes. In fig. 7c we plot the power spectral density for the cell with the larger amplitude modulation (i.e. cell 2 in fig. 6b when ordered from the left). In addition to the main peak at $\omega_1 \simeq 0.263$ we find a low frequency peak at $\omega_2 \simeq 0.016$ which corresponds to the slow modulation of the envelope. These two frequencies do not appear to be related to each other by a simple rational relation. Since this spectrum is calculated from the maximal temperature of one particular cell, it represents the dynamics in a frame rotating with that cell. In the laboratory frame the rotation rate will add a third frequency to the spectrum. The location of the maxima Θ_i as a function of time is shown in fig. 7d. We note that there is a modulation in position (and thus in velocity) and that the modulations are distinctly different for adjacent cells.

Following the QPMTW branch further by decreasing Le , we find a transition to solutions exhibiting seemingly random creation and annihilation of cells through phase slips. For values of Le near the transition point, the chaotic behavior is characterized by intervals where cells are created and annihilated without undergoing any organized motion, alternating, in a seemingly random fashion, with intervals in which there are 4 cells which undergo a roughly organized motion similar to that of QPMTW solutions. This general type of behavior is qualitatively similar to the intermittently ordered states observed in [30]. We illustrate this behavior in figs. 10a-b where we plot $\Theta(r_*, \psi, t)$ for $Le=0.165$. The figures are sequential and contiguous in t , the data is presented in 2 separate figures for clarity. Note that although a transition to chaos can generally be expected from a branch of quasiperiodic solutions with three independent frequencies [17], here the transition may not be via the quasiperiodic route as a result of symmetries. This is also supported by the fact that phase slips are very important in the chaotic dynamics so that the qualitative features of the chaotic attractor strongly differ from those of the quasiperiodic attractor.

We also find a narrow window in Le in which a fourth branch of stable modulated waves exists. The behavior of solutions along this branch is illustrated in fig. 8 where $\Theta(r_*, \psi, t)$ is plotted for $Le = 0.175$. Again, the shape of the cells is modulated in time. In contrast to the BMTW and QPMTW solutions, however, alternate cells are *in phase*, i.e. the solution has the discrete translation symmetry

$$\Theta(\psi + 2\pi/2, t) = \Theta(\psi, t),$$

which does not involve any phase shifts. Thus the spatial period is only half the system size, as compared to the BMTW solutions which only have the period 2π . We therefore call this new branch a half-period MTW (HPMTW).

Our results indicate that the HPMTW branch bifurcates from the TW4 branch. Since the TW4 solutions have the spatial symmetry

$$\Theta(\psi + 2\pi/4, t) = \Theta(\psi, t), \tag{12}$$

the bifurcation corresponds to a pure period doubling in space. For comparison, the analogous transition from the TW4 branch to the BMTW branch constitutes a period quadrupling. The modulation of the temperature maxima is strictly periodic as can be seen from fig. 9a where the temperature maxima for two adjacent cells are plotted. The angular locations of the 4 maxima are plotted in fig. 9b as a function of time. Note that the rotation direction is reversed from the previous cases. This is an effect of the initial conditions. For each rotating solution, a solution rotating in the opposite direction can easily be obtained by simply reflecting the angular coordinate. We also observe from fig. 9b that the oscillation in peak location is exactly in phase for alternate cells.

The HPMTW branch can be obtained by following the (unstable) TW4 branch, imposing periodicity over the interval $0 \leq \psi \leq \pi$. At onset the HPMTW branch is unstable when considered over the full angular interval $0 \leq \psi \leq 2\pi$. This is expected since it bifurcates from the TW4 branch which is itself unstable for this range of Le . From the computation in the restricted domain we have observed that the subharmonic mode (mode 2) appears to grow continuously from 0 as Le is reduced thus indicating that the HPMTW branch bifurcates from the TW4 branch. In the full domain the HPMTW branch becomes stable for lower values of Le . Both in the restricted and the full domain the HPMTW branch loses stability to an apparently chaotic attractor for Le approximately 0.165. Thus, its range of stability extends beyond that of the QPMTW branch and at $Le = 0.170$ the HPMTW branch coexists stably with an apparently chaotic solution arising from an instability of the QPMTW solutions for Le sufficiently small.

We note that the two successive bifurcations of modulated waves from the TW4 branch (to the BMTW and HPMTW branches, respectively) suggests the possibility of a third bifurcation, to a branch which, extending our notation might be called a quarter period MTW, in which each cell is modulated but all cells are exactly in

phase and satisfy the symmetry (12). In fact the modulated wave reported in [31] appears to satisfy an analogous symmetry (the number of cells was different). An investigation of the TW4 branch for smaller values of Le has failed to find such a branch although it is quite possible that such a branch exists for other parameter values.

5. ANALYSIS. In this section we describe two approaches which yield insight into the connection between the S4, S8 and TW4 branches as well as between the TW4 and PMPY branches, respectively. The merging of the S4 branch with the S8 branch suggests considering the resonant interaction of a mode with amplitude A and wave number q and a mode with amplitude B and wavenumber $2q$ corresponding to S4 and S8, respectively. In the vicinity of a codimension-2 point in parameter space at which both these modes simultaneously destabilize the axisymmetric state the dynamics of the system restricted to $2\pi/4$ periodic solutions can be described by two complex amplitude equations

$$\begin{aligned}\partial_T A &= \mu_1 A + c_1 A^* B + a_1 A |A|^2 + b_1 A |B|^2, \\ \partial_T B &= \mu_2 B + c_2 A^2 + b_2 B |A|^2 + a_2 B |B|^2,\end{aligned}\tag{13}$$

where $*$ denotes complex conjugate, and T is a slow time variable. The coefficients a_i , b_i , and c_i are $O(1)$, and μ_1 and μ_2 are the control parameters. These equations, which have been studied extensively, e.g. [1, 23, 46], exhibit a parity-breaking transition from a stationary q mode branch to a TW branch before the q mode branch merges with the $2q$ mode branch, just as in the numerical computations of cellular flames considered here. Though these simulations are not close to such a codimension 2 point, calculations in directional solidification [49] and in Taylor vortex flow [50] showed that the regime of existence of the TW branch can extend far beyond this special point in parameter space. Thus the amplitude equations (13) for the $q : 2q$ mode interaction appear to describe transitions from S4 to TW4 and to S8, respectively. The amplitude equations also describe MTW solutions, but these are different from the MTW solutions described in this paper. This is due to the fact that eqs.(13) are restricted to a description of the behavior of four identical cells, while in our MTW solutions PMPY, BMTW and HPMTW as well as in our QPMTW solution, the four cells do not behave identically.

To understand the stability behavior of solutions on the TW4 branch as well as the relation of the TW4 branch to the PMPY branch, it is useful to take a different approach. In the vicinity of a parity-breaking instability the dynamics can be described by two coupled real equations for the amplitude A of the small antisymmetric part of the solution, which measures the extent to which the reflection symmetry is broken, and the local phase ϕ of the solution, which gives the instantaneous position of each cell [22]. In the context of the present computation the symmetric solution S4 corresponds to $A = 0$ and the asymmetric TW4-solution to $A = A_0 = \text{const}$. In

order to describe the PMPY-solution one would have to allow the asymmetric amplitude to depend on the spatial coordinate. This is systematically possible only in the limit that the spatial variations occur on a long length scale. We therefore imagine introducing the radius R of the circular flame front as an additional parameter which can be changed by changing the flow rate κ . In the limit $R \rightarrow \infty$ the introduction of a slow angular coordinate $X = \epsilon\psi$ and a slow time variable $T = \epsilon t$, $\epsilon \ll 1$, on which A and ϕ are allowed to depend, is justified and one can find evolution equations for A and ϕ . One may hope, that these equations then also describe the system with finite R in a qualitative way. Strikingly, this is indeed the case as is shown below.

To derive the evolution equations for the amplitude A of the asymmetric part and the local phase ϕ we expand the physical variable, say u , as

$$u = u_S(\phi) + \epsilon A(X, T)u_A(\phi) + h.o.t.,$$

and use symmetry and scaling arguments to obtain the evolution equations [20, 22]

$$\begin{aligned} \partial_T \phi &= A, \\ \partial_T A &= \lambda_1 \partial_X \phi A + b_2 \partial_{XX} \phi \\ &+ \epsilon \left\{ (\lambda_0 + \lambda_2 (\partial_X \phi)^2) A + d_2 \partial_{XX} A - A^3 + g A \partial_X A + b_{21} \partial_X \phi \partial_{XX} \phi \right\}. \end{aligned} \quad (14)$$

Note that the equations explicitly contain ϵ which signifies that, strictly speaking, two separate slow time scales may be called for. Instead, we consider the reconstituted equations and keep track of the relative order of the terms as signified by ϵ . Extended traveling wave solutions, which we associate with TW4 solutions, are given by

$$A^2 = \lambda_0 \equiv A_0^2, \quad \phi_0 = \omega T \quad (15)$$

with $\omega = A_0$. In general, ϕ could also have a linear dependence on X , but it can be absorbed into the coefficients λ_1 , λ_2 and b_{21} . To determine the linear stability of this solution we write it as

$$A = A_0 + \delta A_1 e^{ipx + \sigma t}, \quad \phi = \phi_0 + \delta \phi_1 e^{ipx + \sigma t}. \quad (16)$$

Inserting into (14) and linearizing in $\delta \ll 1$ yields the dispersion relation

$$\sigma^2 + \epsilon \sigma \left(2A_0^2 + d_2 p^2 - ipg A_0 \right) + b_2 p^2 - ip A_0 \lambda_1 = 0. \quad (17)$$

Using the Hurwitz criterion, the TW solutions are stable iff

$$d_2 > 0 \quad (18)$$

and

$$\begin{aligned} H(p, A_0) &\equiv b_2 d_2^2 p^4 + p^2 d_2 A_0^2 (4b_2 + \lambda_1 g) \\ &+ 2\lambda_1 g A_0^4 + 4b_2 A_0^4 - \lambda_1^2 A_0^2 \epsilon^{-2} > 0. \end{aligned} \quad (19)$$

Thus, stability with respect to perturbations with large wave numbers p (short waves) requires $b_2 > 0$, which is also a condition for the stationary structure described by $A = 0$ to be Eckhaus-stable. If $b_2 < 0$, a fourth derivative of ϕ must be included in (14), as in (25) below, in order to obtain a well posed problem. Strikingly, if ϵ is small, traveling wave solutions are unstable to long wavelength perturbations due to the term involving λ_1 [20]. That is, for ϵ and p small, (19) cannot be satisfied. Thus, in an infinite system, which allows $p \rightarrow 0$, i.e., allows very long-wave perturbations, the traveling waves are in general *unstable at onset* if $\lambda_1 \neq 0$. Since λ_1 determines the slope of the neutral stability curve corresponding to the secondary bifurcation, this stability behavior is similar to that of stationary structures which arise in a primary bifurcation; there, only the structure with the critical wavenumber (at the minimum of the neutral curve, where the analog of λ_1 is 0) is stable at onset with respect to the Eckhaus instability. States with other wave numbers can become stable further above threshold. By analogy, we might expect that the TW branch could also gain stability at larger amplitudes, even if $\lambda_1 \neq 0$. This can be seen by assuming λ_1 to be small,

$$\lambda_1 = \epsilon \Lambda_1. \quad (20)$$

Since H is strictly increasing with p^2 , the TW solutions become stable in an infinite system when $H(p = 0) = 0$, i.e. for

$$A_0^2 \geq \frac{\Lambda_1^2}{4b_2}. \quad (21)$$

The TW branch $A^2 = \lambda_0$ arises through a supercritical pitchfork bifurcation. In a finite system with periodic boundary conditions the bifurcation is also a pitchfork and we therefore expect the TW solutions to be stable even at onset, since only a single real eigenvalue passes through 0. The eigenvalue corresponding to the translation mode is identically zero and, since the spectrum is discrete, the remaining eigenvalues are in the left half plane, bounded away from the imaginary axis. This result can be recovered from (19) by limiting p to $p \geq p_c \equiv 2\pi/L$ where L is the length of the system. Then for small ϵ the TW branch is stable in two windows given by

$$A < \frac{1}{4} \sqrt{\frac{\Lambda_1^2}{b_2}} \left(1 - \sqrt{1 - \frac{8b_2 d_2 4\pi^2}{\Lambda_1^2 L^2}} \right), \quad (22)$$

$$A > \frac{1}{4} \sqrt{\frac{\Lambda_1^2}{b_2}} \left(1 + \sqrt{1 - \frac{8b_2 d_2 4\pi^2}{\Lambda_1^2 L^2}} \right). \quad (23)$$

The TW branch becomes stable for all amplitudes, i.e., the window of instability disappears, if

$$L^2 < \frac{32b_2 d_2 \pi^2}{\Lambda_1^2}. \quad (24)$$

Based on (20) we might therefore expect that the TW solution is stable at onset.

In contrast to this argument, in the numerical computation of (1) the TW4 branch seems to be unstable as close to onset as could be investigated. In addition, the stationary S4 branch appears to be stable all the way to the parity-breaking bifurcation, beyond which, presumably due to the Eckhaus instability, perturbations evolve to the S5 branch. We therefore consider the case that the parity-breaking instability and the Eckhaus instability ($b_2 = 0$) occur extremely close to one another. Such a situation occurred in Taylor vortex flow [50]. Thus we extend equations (14) to the case $b_2 = \epsilon^2\beta$ and allow β to have either sign depending on which bifurcation occurs first. This leads to

$$\begin{aligned}\partial_T\phi &= A, \\ \partial_TA &= \lambda_1\partial_X\phi A \\ &\quad + \epsilon \left\{ (\lambda_0 + \lambda_2 (\partial_X\phi)^2)A + d_2\partial_X^2 A - A^3 + gA\partial_X A + b_{21}\partial_X\phi\partial_X^2\phi \right\} \\ &\quad + \epsilon^2 \left\{ \beta\partial_X^2\phi - b_4\partial_X^4\phi \right\}.\end{aligned}\tag{25}$$

Note that we assume $b_4 > 0$ for well posedness. Taking $\lambda_1 = \epsilon^2\Lambda_1$ leads to

$$\begin{aligned}H &= \left(4(\beta + b_4p^2) + 2\Lambda_1g\right) A_0^4 \\ &\quad + \left(d_2p^2(4\beta + 4b_4p^2 + \Lambda_1g) - \Lambda_1^2\right) A_0^2 + d_2^2p^4 (\beta + b_4p^2).\end{aligned}\tag{26}$$

Thus, for small amplitudes the TW solutions are unstable to long-wavelength perturbations $p^2 < -b_4/\beta$, as in the stationary structure. However, for larger amplitudes the unstable TW solutions become stable if

$$\Lambda_1g > -2\beta > 0.\tag{27}$$

Thus, with $\beta < 0$ the above scenario describes a TW branch which is unstable at onset but stabilizes at some distance from onset, as found in the numerical computation of (1).

The coupled phase-amplitude equations (25) also give insight into the PMPY solution discussed in section 4. The PMPY solutions can be described as a localized wave of asymmetry traveling through the underlying symmetric array of stationary cells. For the case $b_2 > 0$, for which the stationary cells are Eckhaus-stable, it has been shown that (14) supports stable solutions of that kind [20, 50]. Their existence can be seen easily in the special case $g = b_{21} = \lambda_2 = 0$ [50]. After introducing $q = \partial_X\phi$ and going into a frame moving with velocity v , (14) can be solved for q , as

$$q = -A/v + q_\infty.\tag{28}$$

For stationary solutions this leads to an ‘equation of motion for a particle with mass d_2 ’,

$$d_2\partial_X^2 A + \left(v - \frac{b_2}{v}\right) \partial_X A = -\partial_A U(A)\tag{29}$$

in the ‘potential’

$$U(A) = \frac{1}{2}(\epsilon\lambda_0 + \lambda_1 q_\infty)A^2 - \frac{1}{3}\frac{\lambda_1}{v}A^3 - \frac{\epsilon}{4}A^4. \quad (30)$$

Localized solutions correspond to homoclinic orbits of (29) which start at the maximum of the potential at $A = 0$ for $X = -\infty$, reach a turning point at A_{max} and return to $A = 0$ for $X = \infty$. Such orbits exist if the ‘friction’ $v - \frac{b_2}{v}$ vanishes and if $\lambda_0 \geq \lambda_c \equiv -\lambda_1/\epsilon(2\lambda_1/(9\epsilon b_2) + q_\infty)$. The latter condition ensures that the value of the potential at its second maximum, which occurs at nonzero A , is positive and therefore above the value at the turning point A_{max} , $U(A_{max}) = 0$.

Since the numerical calculations in section 4 strongly suggest that the stationary structure becomes Eckhaus-unstable very close to the parity-breaking bifurcation, the analysis of (14) is not sufficient. Applying a similar analysis to the extended eqs.(25) leads to an integral condition for the determination of v , given by

$$\int_{-\infty}^{\infty} \partial_X A \left(\left(\frac{\epsilon b_{21}}{v^2} + \epsilon g \right) A \partial_X A + \left(v - \frac{b_2}{v} - \frac{\epsilon b_{21} q_\infty}{v} \right) \partial_X A + \frac{\epsilon^2 b_4}{v} \partial_X^3 A \right) dX = 0, \quad (31)$$

which replaces the condition $v - b_2/v = 0$. This condition expresses the statement that there is no change in the total ‘energy’ along the homoclinic orbit. Instead of treating this condition together with the equation of motion by perturbation methods [20], we solve (25) numerically, which, in addition to showing the existence of such localized solutions, will also show their stability, at least for the given parameter values.

Localized waves behave like a symmetric stationary state ($A = 0$) for $X \rightarrow \pm\infty$, i.e. for $q \rightarrow q_\infty$, and like an asymmetric traveling wave ($A^2 = \lambda_0$) in a localized region. From (28) with $A^2 = \lambda_0$ the wave number in the asymmetric region is $q_{as} \neq q_\infty$. We would like to determine parameter values for use in the numerical solution of (25), to exhibit stable localized waves. Thus we would like to determine conditions on the parameter values to insure that the symmetric stationary state is stable for $X \rightarrow \pm\infty$ ($q \rightarrow q_\infty$), and that the asymmetric traveling wave is stable for X in the asymmetric region ($q = q_{as}$). It is simpler to determine conditions that insure that the symmetric stationary and the asymmetric traveling wave solutions, each defined on the entire X interval, are simultaneously stable. These conditions then provide an estimate for the parameter values to be used in (25). For the stability of the symmetric stationary state we require

$$b_2 + b_{21}q_\infty > 0, \quad d_2 > 0, \quad \lambda_1 q_\infty + \epsilon(\lambda_0 + \lambda_2 q_\infty^2) < 0, \quad (32)$$

where the first condition corresponds to the condition $b_2 > 0$ given above, with the role of b_2 played by $b_2 + b_{21}q_\infty$, and the third condition follows from the requirement

that the growth rate (coefficient of the term linear in A in (25)) is negative. For the stability of the asymmetric traveling wave we choose g to satisfy

$$\Lambda_1 g > -2(b_2 + b_{21}q_{as}) > 0, \quad (33)$$

which is the analog of (27), where now $b_2 + b_{21}q_{as}$ plays the role of b_2 . Thus, though the stationary state at the local wave number q_{as} would be Eckhaus-unstable since $b_2 + b_{21}q_{as} < 0$, the traveling wave can be stable due to the presence of the nonlinear gradient term $gA\partial_X A$. Fig. 11a shows the temporal evolution of A for such a stable localized wave with $\lambda_0 = -0.1$, $\lambda_1 = -3$, $\lambda_2 = 0$, $d_2 = 1$, $b_2 = 0$, $b_{21} = 0.1$, $b_4 = 1$ and $g = -0.5$. In fig. 11b the amplitude and the wave number are shown for a representative time.

Unfortunately, the coefficients for (14) are not known for the system of interest here. Thus, a quantitative comparison is not possible. The above calculations show, however, that these equations may very well describe the behavior of the cellular flames in the vicinity of the parity-breaking bifurcation.

ACKNOWLEDGMENTS. This work was supported by N.S.F. grants MSS 91-02981 and DMS 90-20289 and D.O.E. grants DE-FG02-87ER25027 and DE-FG02-92ER14303. We are pleased to acknowledge useful discussions with M. Golubitsky, M. Gorman and I. Kevrekidis.

References

- [1] D. Armbruster, J. Guckenheimer and P. Holmes, *Heteroclinic cycles and modulated travelling waves in systems with $O(2)$ symmetry*, Physica D **29** (1988), 257-282.
- [2] D. G. Aronson, M. Golubitsky and J. Mallet-Paret, *Ponies on a merry-go-round in large arrays of josephson junctions*, Nonlinearity **4** (1991), 903-910.
- [3] A. Bayliss, D. Gottlieb, B. J. Matkowsky, and M. Minkoff, *An adaptive pseudo-spectral method for reaction diffusion problems*, J. Comput. Phys. **81** (1989), 421-443.
- [4] A. Bayliss, R. Kuske and B. J. Matkowsky, *A two-dimensional adaptive pseudo-spectral method*, J. Comput. Phys. **91** (1990), 174-196.
- [5] A. Bayliss and B. J. Matkowsky, *Fronts, relaxation oscillations, and period doubling in solid fuel combustion*, J. Comput. Phys. **71** (1987), 147-168.
- [6] A. Bayliss and B. J. Matkowsky, *Spinning cellular flames*, Appl. Math. Lett. **3** (1990), 75-79.
- [7] A. Bayliss and B. J. Matkowsky, *Bifurcation pattern formation and chaos in combustion*, in “Dynamical Issues in Combustion Theory”, P. Fife, A. Linan and F. Williams eds., Springer-Verlag (1991) 1-36. Proceedings on Dynamical Issues in Combustion Theory.
- [8] A. Bayliss and B. J. Matkowsky, *Bifurcation pattern formation and transition to chaos in combustion*, in “Bifurcation and Chaos: Analysis, Algorithms, Applications”, R. Seydel, F. Schneider, T. Kupper and H. Troger eds., Birkhäuser, Basel (1991), 36-51.
- [9] A. Bayliss and B. J. Matkowsky, *Nonlinear dynamics of cellular flames*, SIAM J. Appl. Math., **52** (1992), 396-415.
- [10] A. Bayliss and B. J. Matkowsky, *From traveling waves to chaos in combustion*, to appear, SIAM J. Appl. Math..
- [11] A. Bayliss, B. J. Matkowsky and M. Minkoff, *Adaptive pseudo-spectral computation of cellular flames stabilized by a point source*, Appl. Math. Lett. **1** (1987), 19-24.
- [12] A. Bayliss, B. J. Matkowsky and M. Minkoff, *Cascading cellular flames*, SIAM J. Appl. Math. **49** (1989), 1421- 1432.

- [13] A. Bayliss, B. J. Matkowsky and M. Minkoff, *Numerical computation of bifurcation phenomena and pattern formation in combustion*, in “Numerical Combustion”, A. Dervieux and B. Larrouturou eds., Lecture Notes in Physics 351 , Springer-Verlag, Heidelberg (1989), 187-198.
- [14] A. Bayliss, B. J. Matkowsky and H. Riecke, *Modulated traveling waves in combustion*, in Numerical Methods for PDEs with Critical Parameters, eds. H. G. Kaper and M. Garbey, Kluwer, Dordrecht (1992), 137-162.
- [15] A. Bayliss and E. Turkel, *Mappings and accuracy for Chebyshev pseudo-spectral approximations*, J. Comput. Phys. **101** (1992), 349-359.
- [16] C.M. Bender and S.A. Orszag, *Advanced Mathematical Methods for Scientists and Engineers* McGraw Hill, New York, (1978).
- [17] P. Berge, Y. Pomeau and C. Vidal, *Order within Chaos*, John Wiley & Sons, N. Y. (1984).
- [18] H.S. Brown and I.G. Kevrekidis, *A computer assisted study of modulated travelling waves in the Kuramoto- Sivashinsky equations*, to appear in Proceedings of the Workshop of Applications of Pattern Formation, J. Chadam, W. Langford and B. Wetton eds., Fields Institute for Research in Mathematical Sciences, (1993).
- [19] C. Canuto, M. Y. Hussaini, A Quarteroni and T. A. Zang, *Spectral Methods in Fluid Dynamics*, Springer-Verlag, New York, (1987).
- [20] B. Caroli, C. Caroli and S.Fauve, *On the Phenomenology of Tilted Domains in Lamellar Eutectic Growth*, J. Phys. **I 2** (1992), 281-290.
- [21] K. T. Coughlin and P. S. Marcus, *Modulated waves in Taylor-Couette flow Part 2. Numerical simulation*, J. Fluid Mech. **234** (1992), 19-46.
- [22] P. Couillet, R.E. Goldstein and G.H. Gunaratne, *Parity-breaking transitions of modulated patterns in hydrodynamic systems*, Phys. Rev. Lett. **63** (1989), 1954-1957.
- [23] G. Dangelmayr, *Steady-state mode interactions in the presence of $O(2)$ -symmetry*, Dyn. Stab. Sys. **1** (1986), 159-185.
- [24] M. el-Hamdi, M. Gorman, J. W. Mapp and J. I. Blackshear Jr., *Stability boundaries of periodic modes of propagation in burner-stabilized methane-air flames*, Comb. Sci. and Tech. **55** (1987), 33-40.
- [25] M. el-Hamdi, M. Gorman and K. A. Robbins, *A picture book of dynamical modes of flat, laminar premixed flames*, Technical Report #2, University of Houston (1990).

- [26] J.M. Flesselles, A.J. Simon and A. Libchaber, *Dynamics of one-dimensional interfaces: an experimentalist's view*, Adv. Phys. **40** (1991), 1.
- [27] M. Garbey, H. A. Kaper, G. K. Leaf and B. J. Matkowsky, *Linear stability analysis of cylindrical flames*, Quarterly of Applied Math. **47** (1989), 691-704.
- [28] M. Gorman, M. el-Hamdi and K. A. Robbins, *Experimental observation of ordered states of cellular flames*, preprint.
- [29] M. Gorman, M. el-Hamdi and K. A. Robbins, *Hopping motion of ordered states of cellular flames*, preprint.
- [30] M. Gorman, M. el-Hamdi and K. A. Robbins, *Four types of chaotic dynamics in cellular flames*, preprint.
- [31] M. Gorman, C. F. Hamill, M. el-Hamdi and K. A. Robbins, *Rotating and modulated rotating states of cellular flames*, preprint.
- [32] M. Gorman and H. L. Swinney, *Spatial and temporal characteristics of modulated waves in the circular Couette system*, J. Fluid Mech. **117** (1982), 123-142.
- [33] D. Gottlieb and S. A. Orszag, *Numerical Analysis of Spectral Methods: Theory and Applications*, C.B.M.S. - N.S.F. Conference Series in Applied Mathematics, SIAM, Philadelphia, (1977).
- [34] J. Kevorkian and J. D. Cole, *Perturbation Methods in Applied Mathematics*, Springer-Verlag, New York, (1981).
- [35] R. Kuske and B. J. Matkowsky, *Two dimensional cellular burner stabilized flames*, Quart. Appl. Math., to appear.
- [36] H. Lofting, *The Voyages of Doctor Dolittle*, J.B. Lippincott, Philadelphia, (1922).
- [37] S. B. Margolis and B. J. Matkowsky, *Nonlinear stability and bifurcations in the transition from laminar to turbulent flame propagation*, Comb. Sci. and Tech. **34** (1983), 45-77.
- [38] G. H. Markstein, ed., *Nonsteady Flame Propagation*, Pergamon Press, Elmsford, NY (1967).
- [39] B. J. Matkowsky and D. O. Olagunju, *Traveling waves along the front of a pulsating flame*, SIAM J. Appl. Math. **42** (1982), 486-501.
- [40] B. J. Matkowsky, and D. O. Olagunju, *Spinning waves in gaseous combustion*, SIAM J. Appl. Math. **42** (1982), 1138-1156.
- [41] B. J. Matkowsky, L. J. Putnick and G. I. Sivashinsky, *A nonlinear theory of cellular flames*, SIAM J. Appl. Math. **38** (1980), 489-504.

- [42] B. J. Matkowsky and G. I. Sivashinsky, *An asymptotic derivation of two models in flame theory associated with the constant density approximation*, SIAM J. Appl. Math. **37** (1979), 686-699.
- [43] D. O. Olagunju and B. J. Matkowsky *Burner-stabilized cellular flames*, Quart. J. Appl. Math. **48** (1990), 645-664.
- [44] D. O. Olagunju and B. J. Matkowsky *Polyhedral flames*, SIAM J. Appl. Math. **51** (1991), 73-89.
- [45] D. O. Olagunju and B. J. Matkowsky *Coupled complex Ginzburg-Landau type equations in gaseous combustion*, , Stab. and Appl. Analysis of Continuous Media **2** (1992), 31-58.
- [46] M.R.E. Proctor and C.A. Jones, *The interaction of two spatially resonant patterns in thermal convection. Part 1. Exact 1:2 resonance*, J. Fluid Mech. **188** (1988), 301-335.
- [47] M. Rabaud, S. Michalland and Y. Couder, *Dynamical regimes of directional viscous fingering: spatiotemporal chaos and wave propagation*, Phys. Rev. Lett. **64** (1990), 184-187.
- [48] D. Rand, *Dynamics and symmetry. Predictions for modulated waves in rotating fluids*, Arch. Rat. Mech. Anal **79** (1982), 1-38.
- [49] W.J. Rappel and H. Riecke, *Parity-breaking in directional solidification: numerics versus amplitude equations*, Phys. Rev. A **45** (1992), 846-859.
- [50] H. Riecke and H.G. Paap, *Parity breaking and Hopf bifurcation in axisymmetric Taylor vortex flow*, Phys. Rev. A **45** (1992), 8605-8610.
- [51] G. I. Sivashinsky, *Instabilities, pattern formation, and turbulence in flames*, Ann. Rev. Fluid Mech. **15** (1983), 179-199.
- [52] R.J. Wiener and D.F. McAlister, *Parity-breaking and solitary waves in axisymmetric Taylor vortex flow*, Phys. Rev. Lett. **69** (1992), 2915-2918.

Figure Captions

Figure 1a. Solution branches as a function of Le .

Figure 1b. Solution branches over restricted region in Le .

Figure 2. Contour plot for Θ for solution on PMPY branch, $Le = 0.42$.

Figure 3. $\Theta(r_*, \psi, t)$ for solution on PMPY branch, $Le = 0.42$, $r_* = 13.5$. Time t (angle ψ) increases along vertical (horizontal) axis.

Figure 4. $\Theta(r_*, \psi, t)$ for solution on BMTW branch, $Le = 0.23$, $r_* = 10.4$. Time t (angle ψ) increases along vertical (horizontal) axis.

Figure 5a. Temperature of two adjacent maxima (peaks) vs. t , for solution on BMTW branch, $Le = 0.27$, $r_* = 11.158$.

Figure 5b. Angular location of temperature maxima (peak) vs. t , for solution on BMTW branch, $Le = 0.27$, $r_* = 11.158$.

Figure 6a. $\Theta(r_*, \psi, t)$ for QPMTW solution, $Le = 0.205$, $r_* = 10.2$. Time t (angle ψ) increases along vertical (horizontal) axis.

Figure 6b. $\Theta(r_*, \psi, t)$ for QPMTW solution, $Le = 0.185$, $r_* = 10.0$. Time t (angle ψ) increases along vertical (horizontal) axis.

Figure 7a. Temperature of two adjacent maxima (peaks) vs. t , for solution on QPMTW branch, $Le = 0.185$, $r_* = 9.842$.

Figure 7b. Temperature of two alternate maxima (peaks) vs. t , for solution on QPMTW branch, $Le = 0.185$, $r_* = 9.842$.

Figure 7c. PSD corresponding to Fig. 7a.

Figure 7d. Angular location of temperature maxima (peaks) vs. t , for solution on QPMTW branch, $Le = 0.185$, $r_* = 9.842$.

Figure 8. $\Theta(r_*, \psi, t)$ for solution on HPMTW branch, $Le = 0.175$, $r_* = 9.8$. Time t (angle ψ) increases along vertical (horizontal) axis.

Figure 9a. Temperature of two adjacent maxima (peaks) vs. t , for solution on HPMTW branch, $Le = 0.175$, $r_* = 9.346$.

Figure 9b. Angular location of temperature maxima (peak) vs. t , for solution on HPMTW branch, $Le = 0.175$, $r_* = 9.346$.

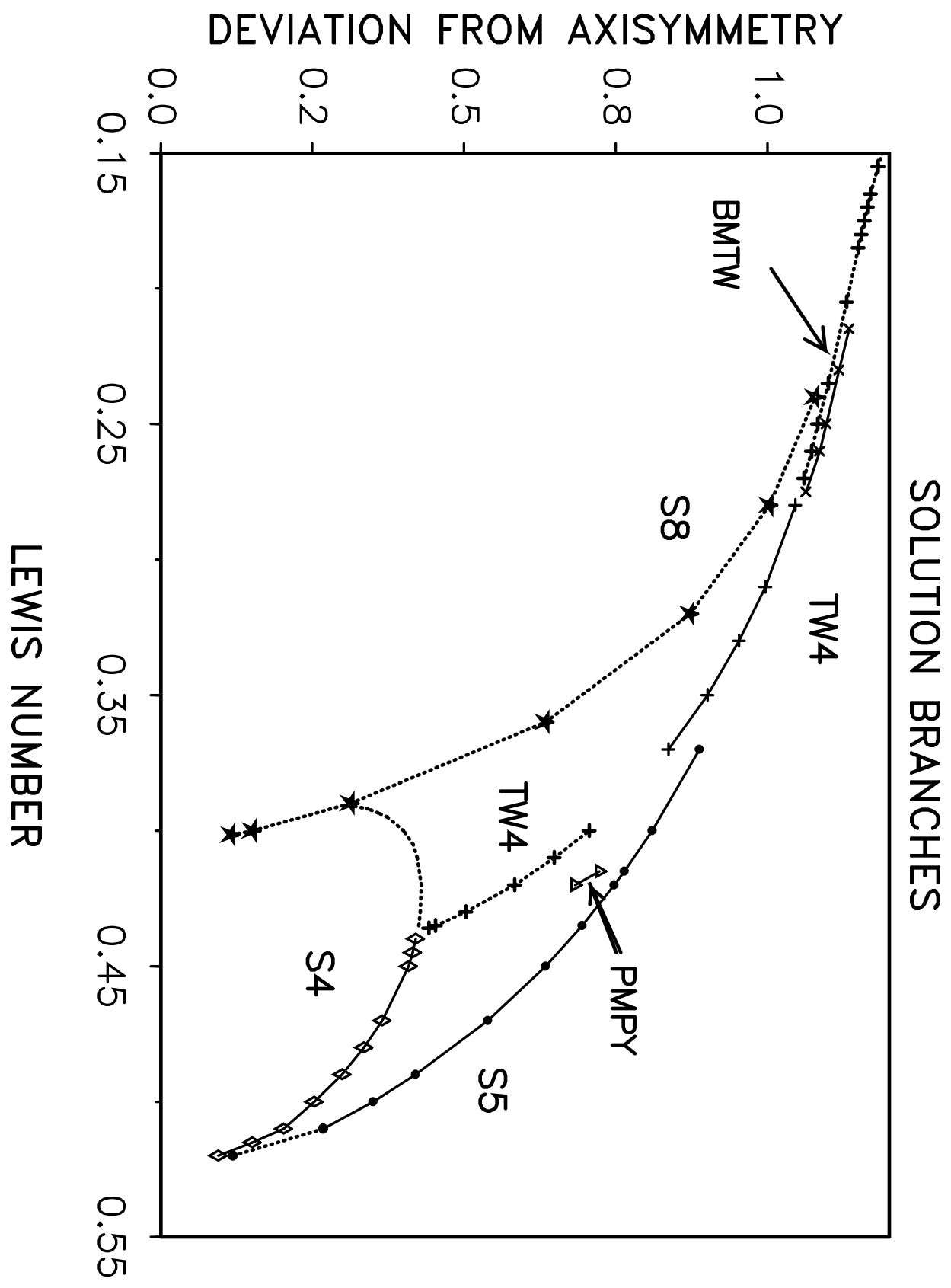
Figure 10a. $\Theta(r_*, \psi, t)$ for solution apparently exhibiting apparently chaotic temporal behavior with a disordered spatial structure, $Le = 0.165$, $r_* = 9.6$. Time t (angle ψ) increases along vertical (horizontal) axis.

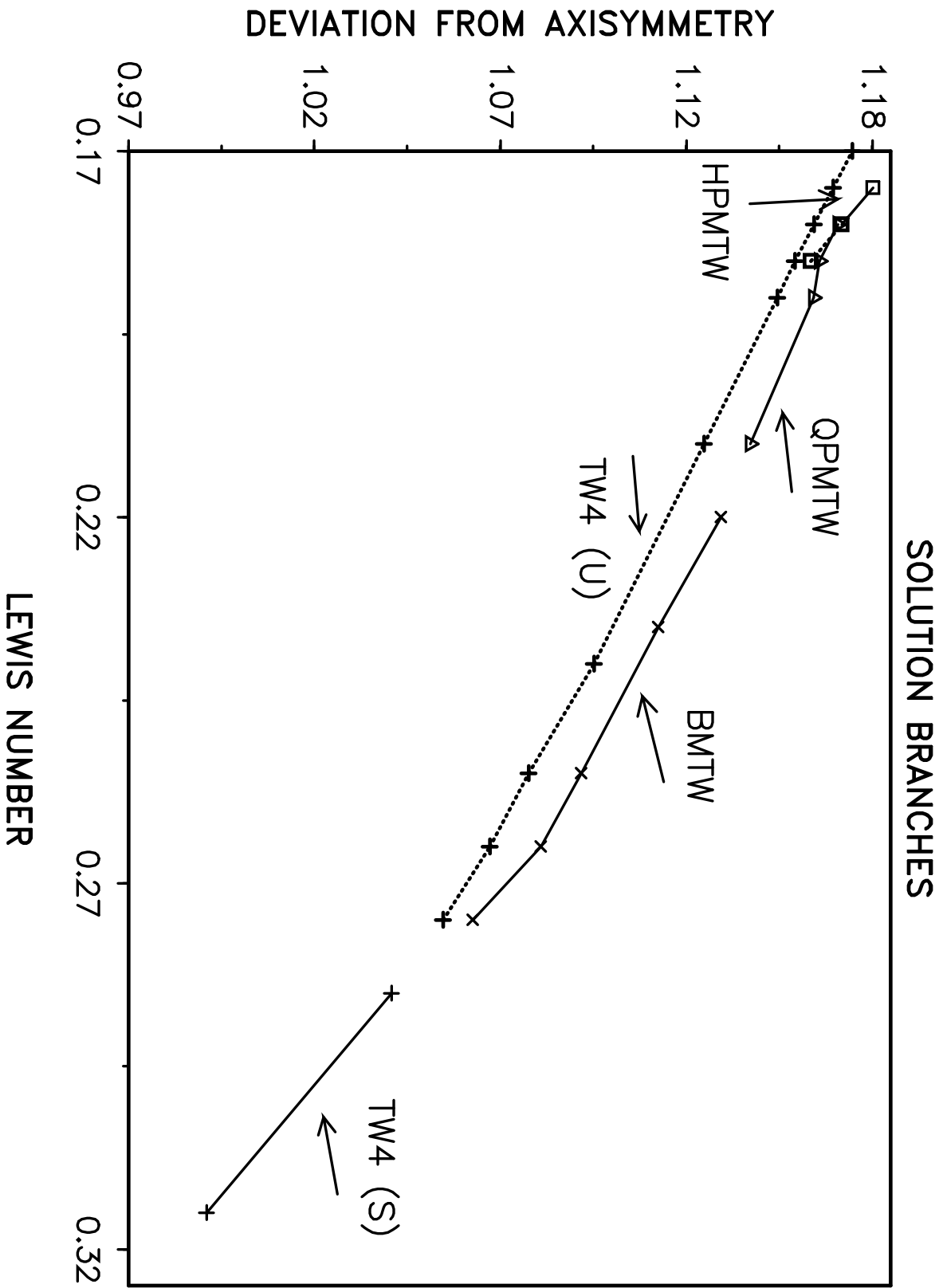
Figure 10b. $\Theta(r_*, \psi, t)$ for solution apparently exhibiting apparently chaotic temporal behavior with a disordered spatial structure, $Le = 0.165$, $r_* = 9.6$. Time t (angle ψ) increases along vertical (horizontal) axis. Continuation of fig. 10a.

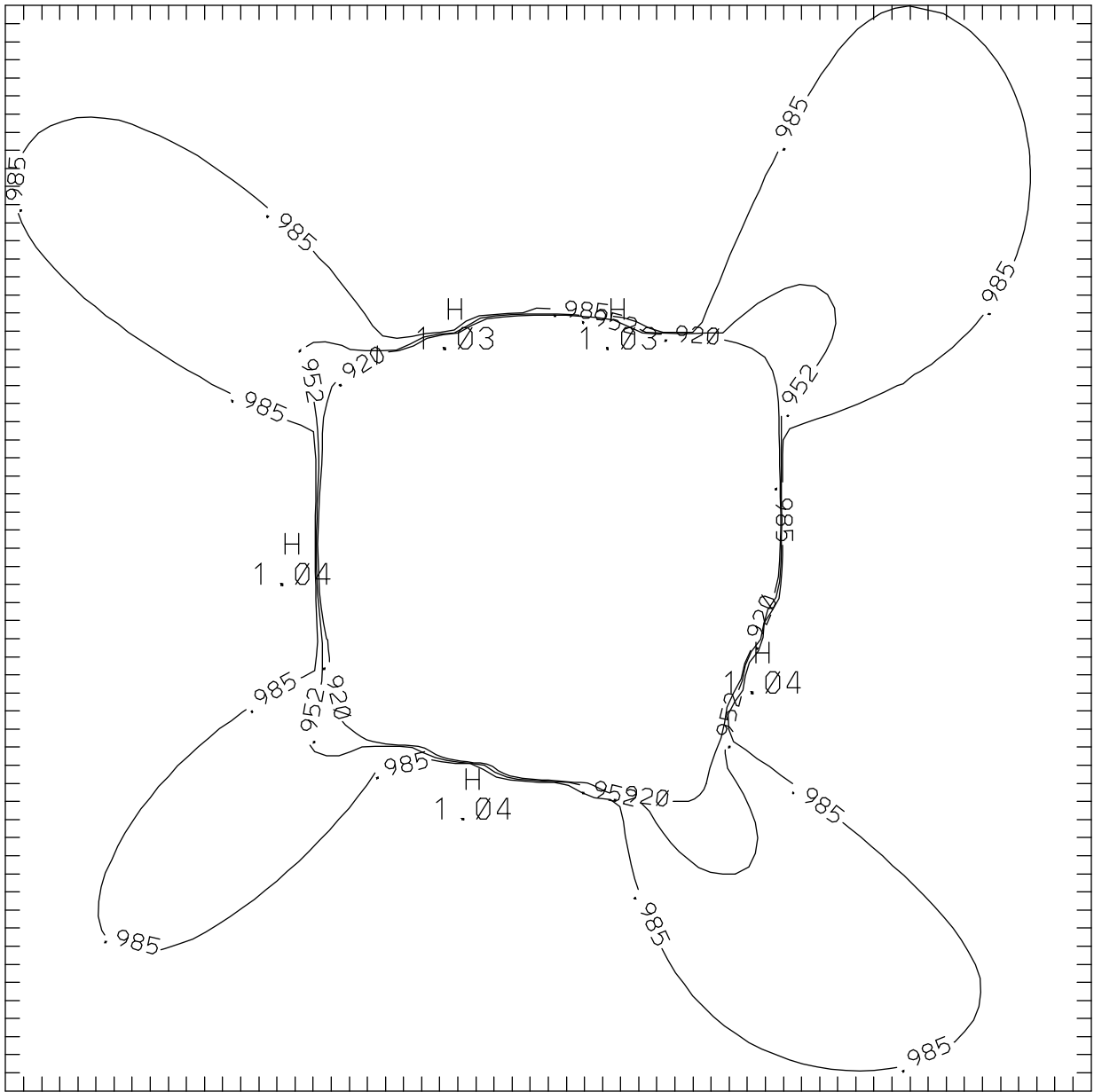
Figure 11.

a) Temporal evolution of asymmetry amplitude A according to phase-amplitude equations (25) for $\lambda_0 = -0.1$, $\lambda_1 = -3$, $\lambda_2 = 0$, $d_2 = 1$, $b_2 = 0$, $b_{21} = 0.1$, $b_4 = 1$ and $g = -0.5$.

b) Representative stable localized wave at same parameters as a).

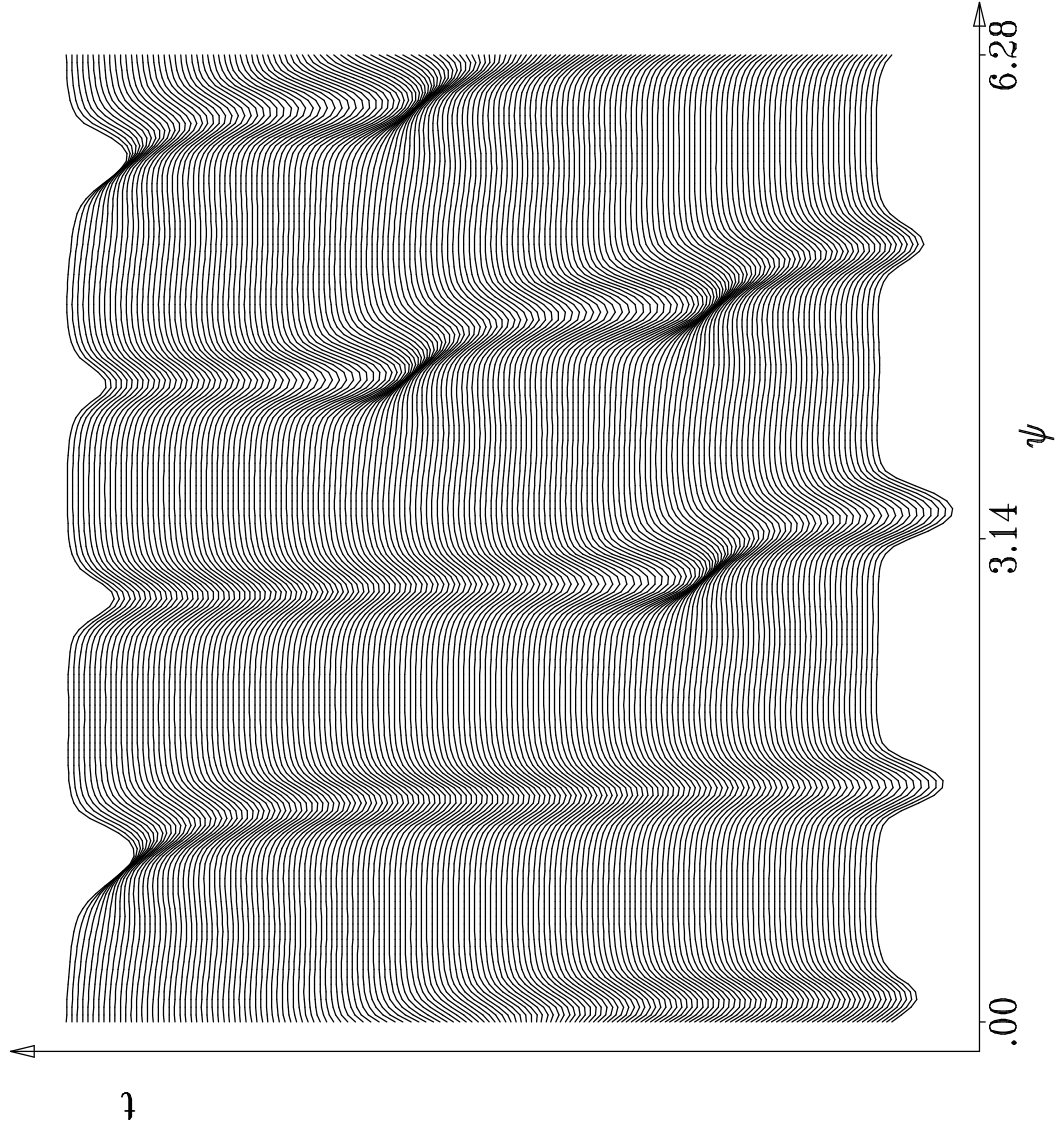




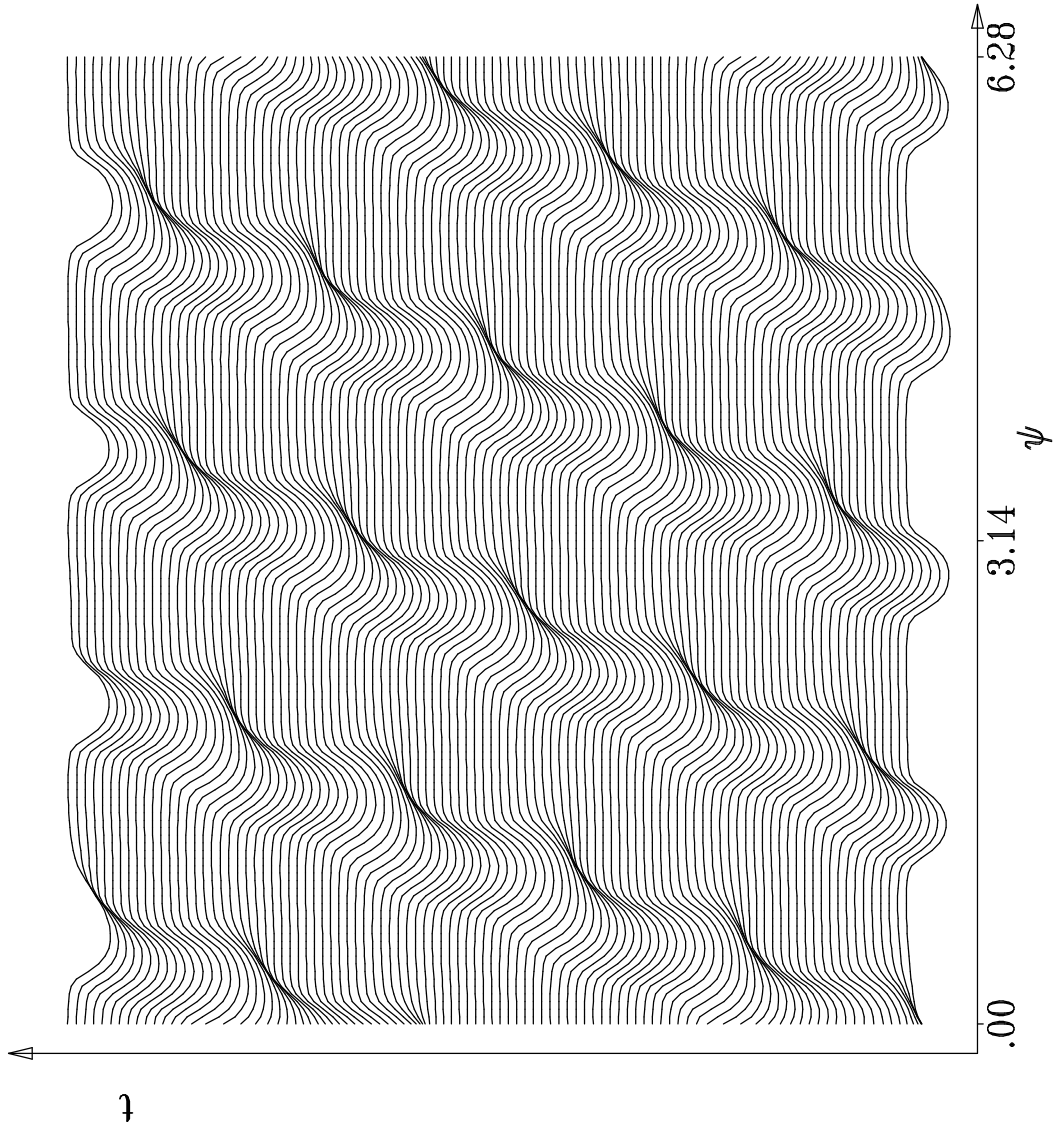


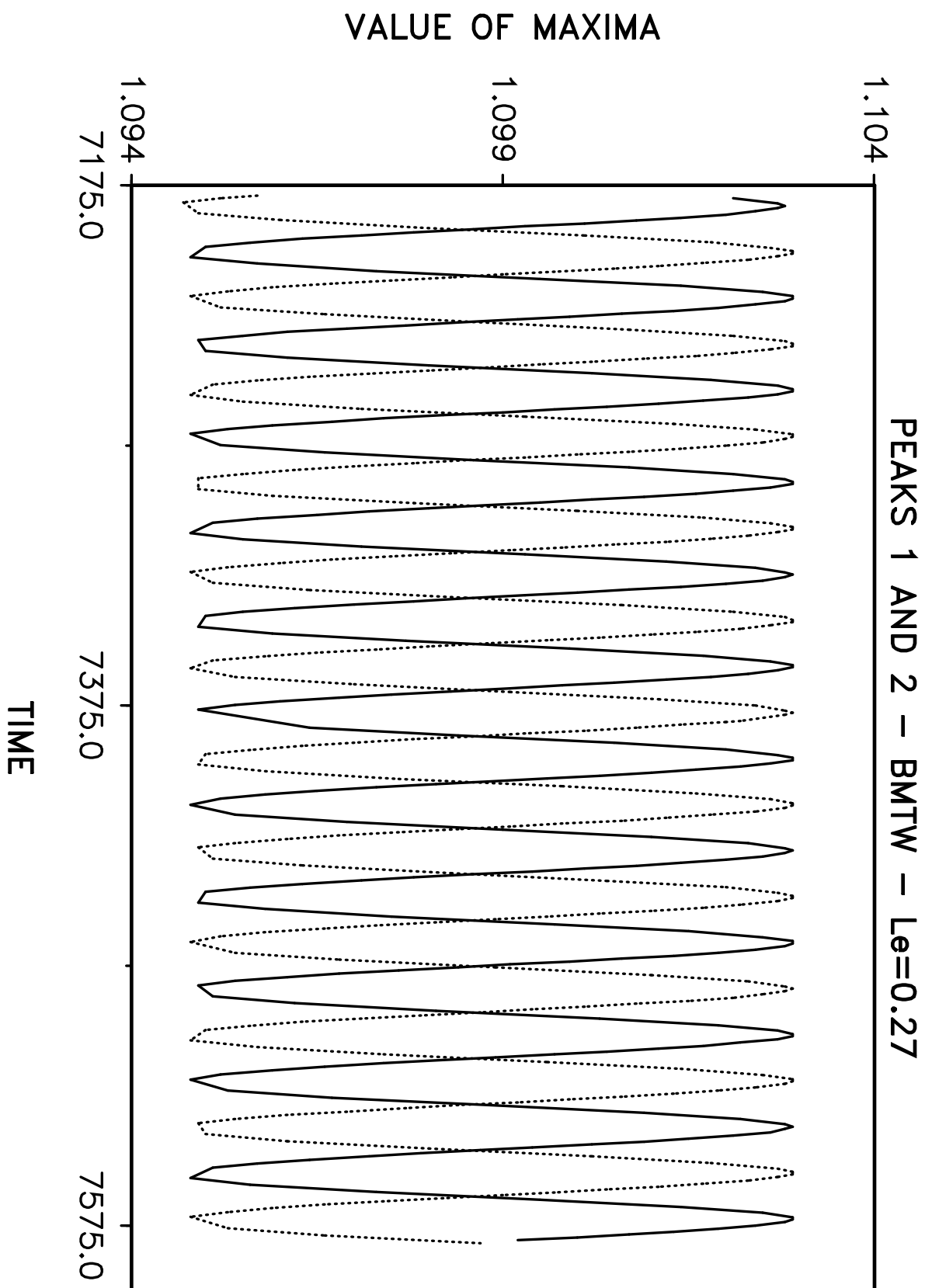
CONTOUR FROM 0.92000 TO 0.98500 CONTOUR INTERVAL OF 0.32500E-01 PT(3,3)= 0.99163

PMPY BRANCH - $Le=0.420$

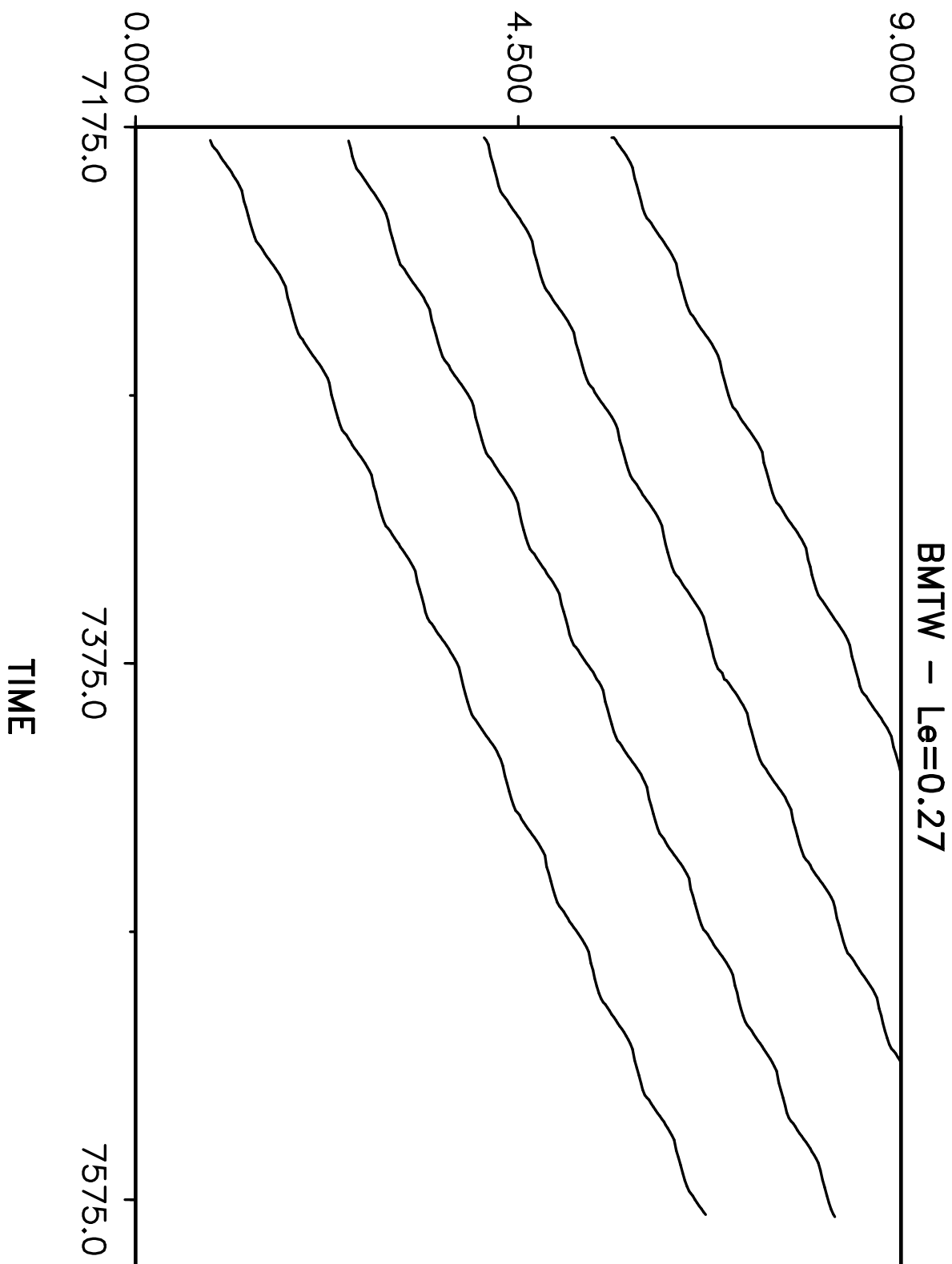


BMTW BRANCH – $Le=0.230$

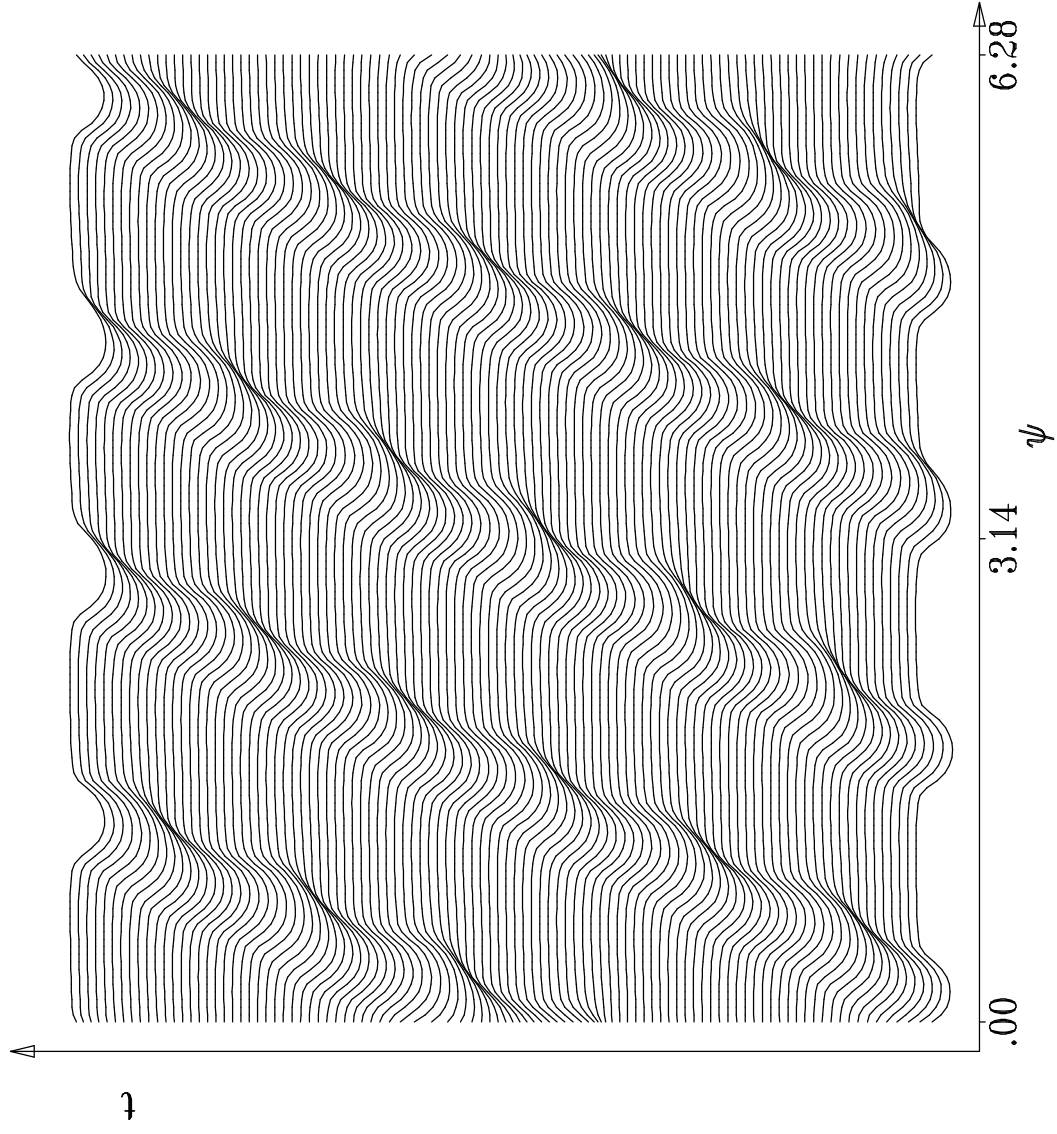




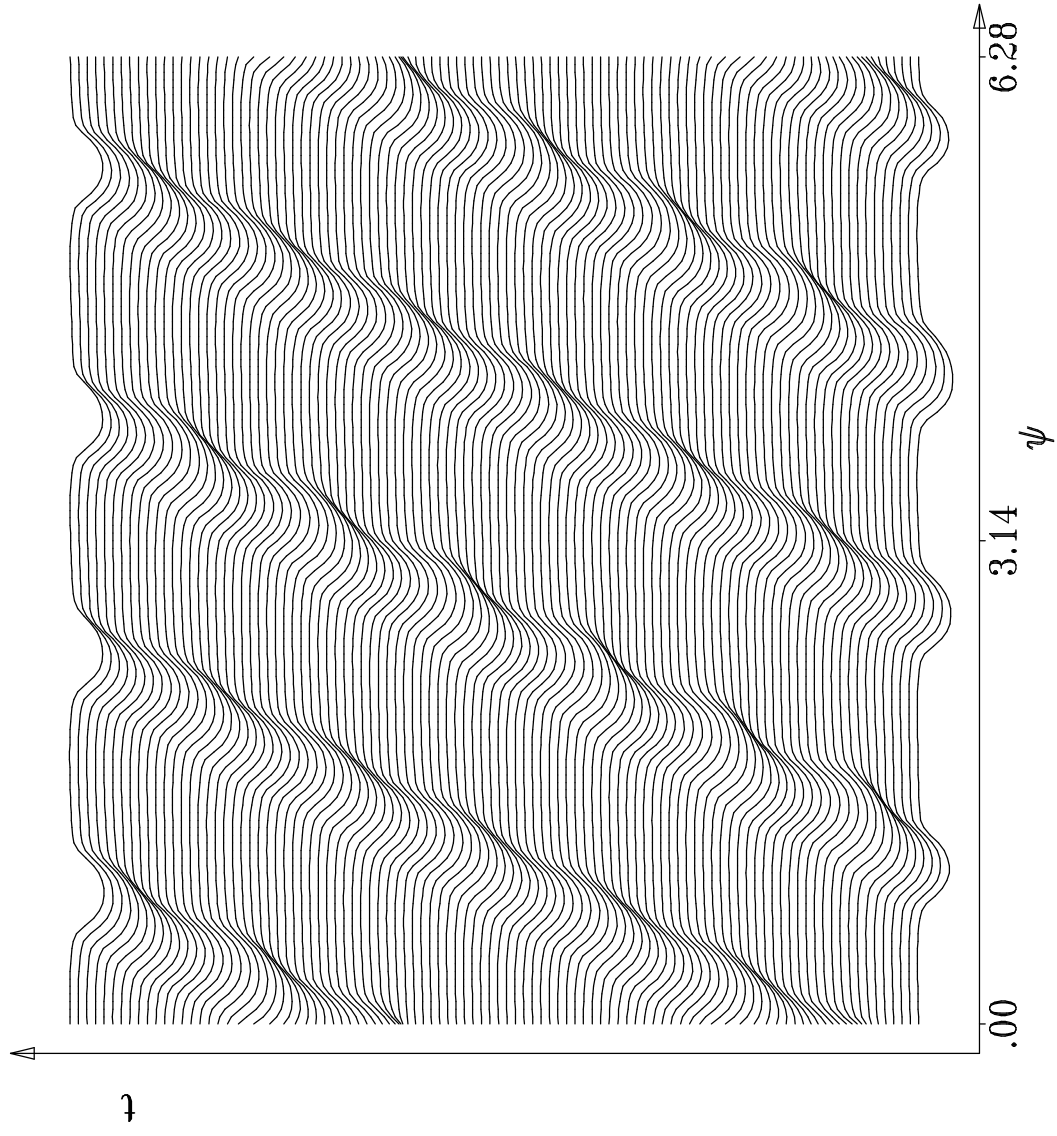
ANGULAR LOCATION OF MAXIMA



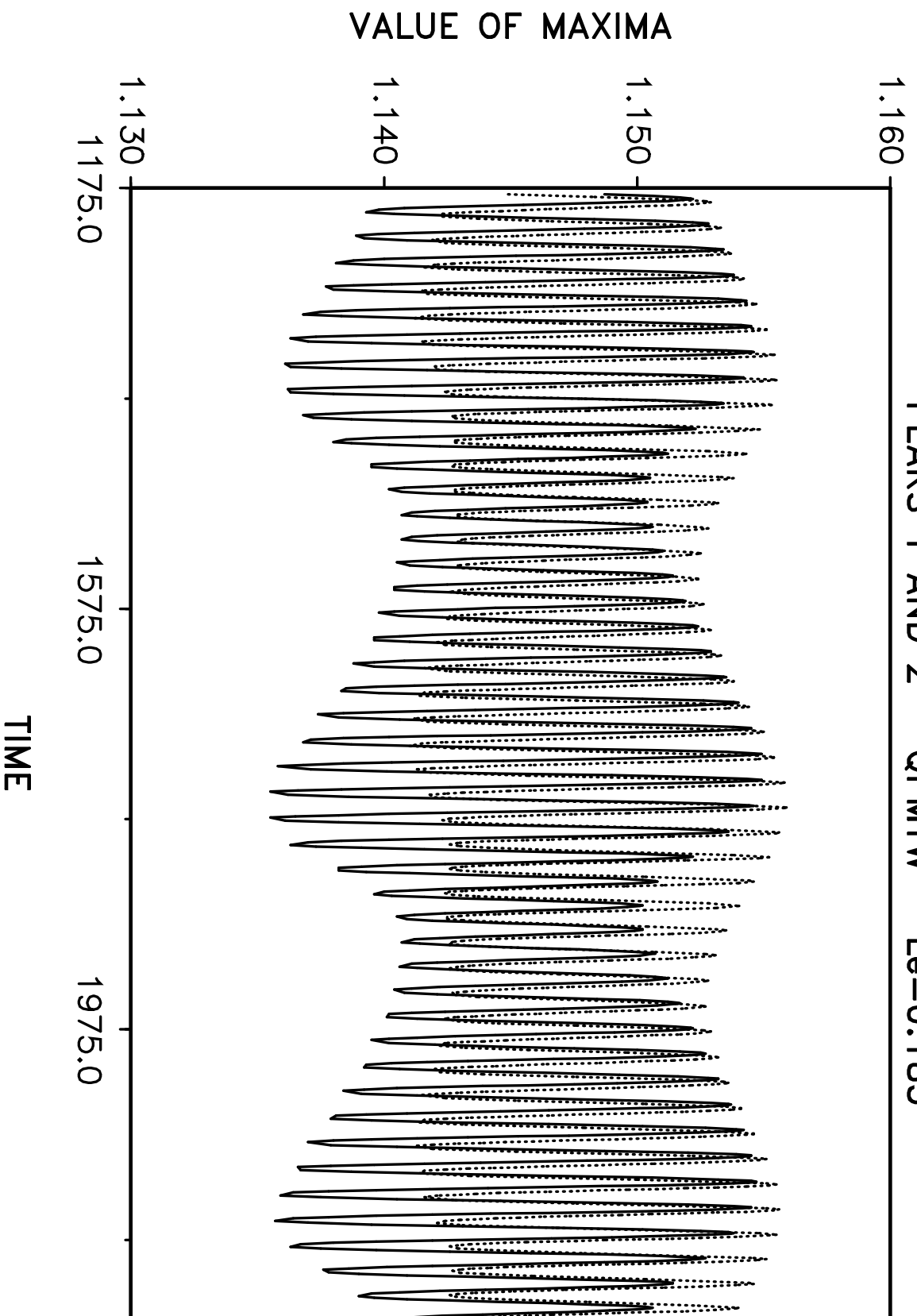
QPMTW BRANCH - $Le=0.205$



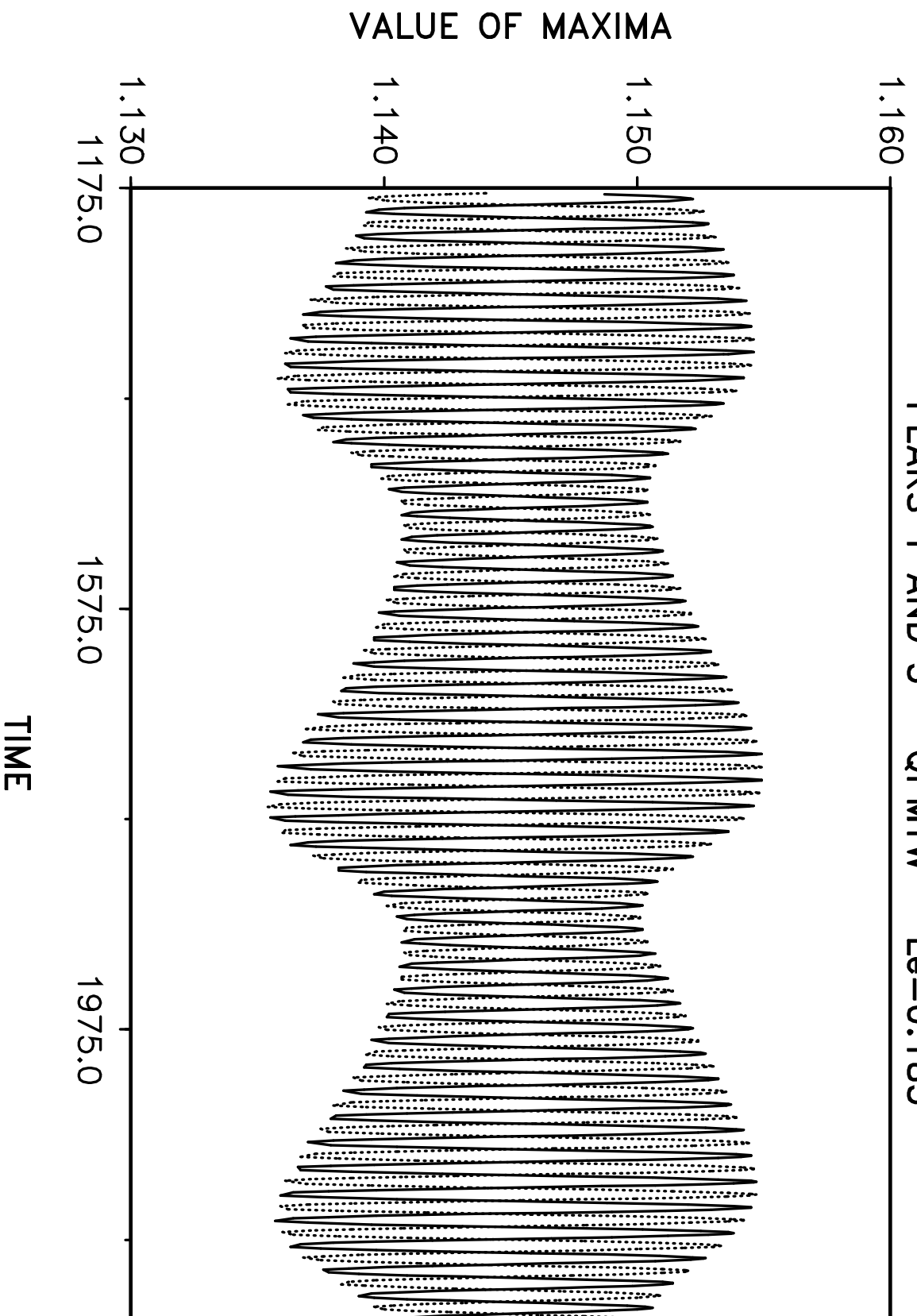
QPMTW BRANCH – $Le=0.185$



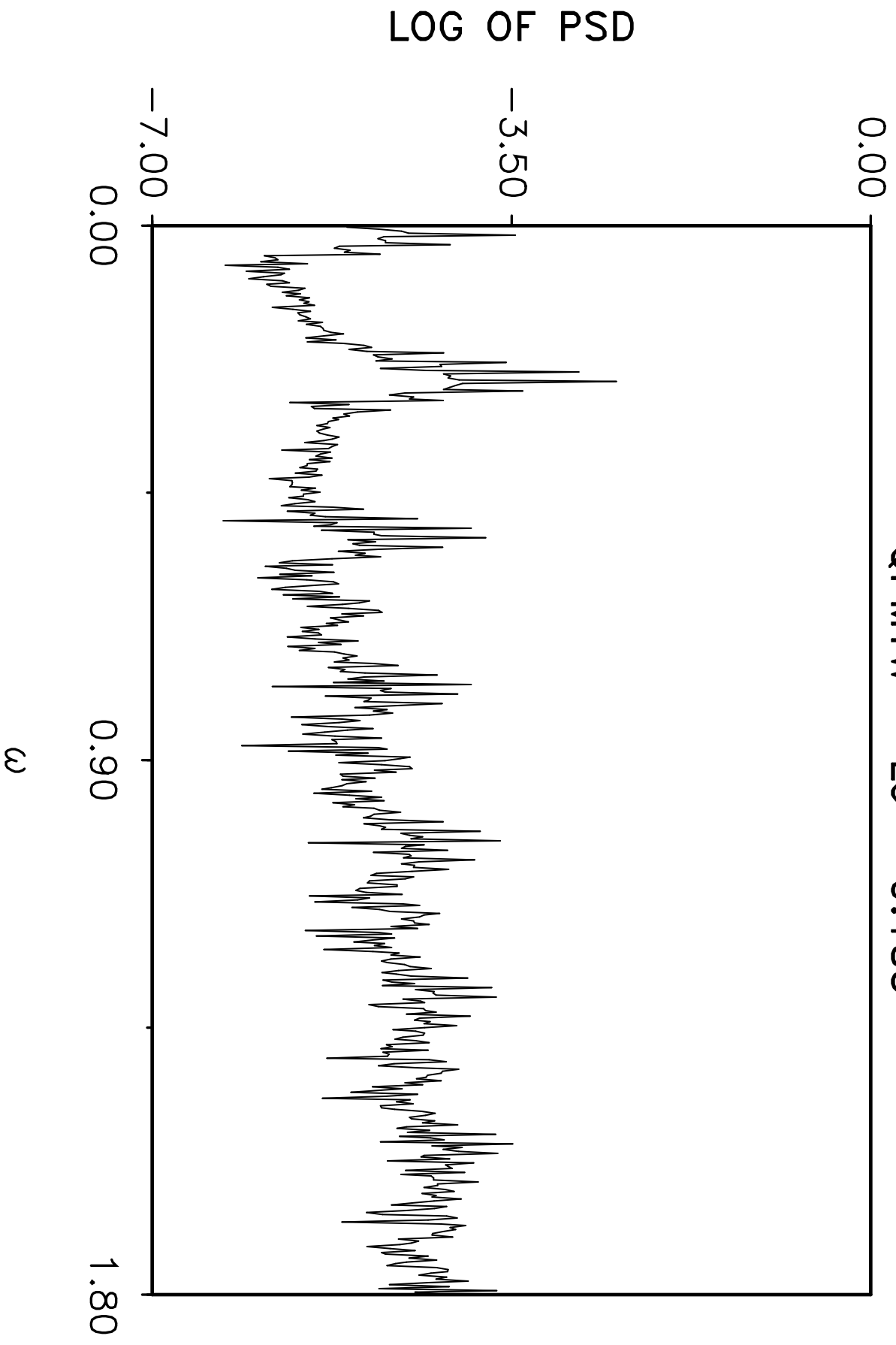
PEAKS 1 AND 2 - QPMTW - Le=0.185



PEAKS 1 AND 3 - QPMTW - Le=0.185

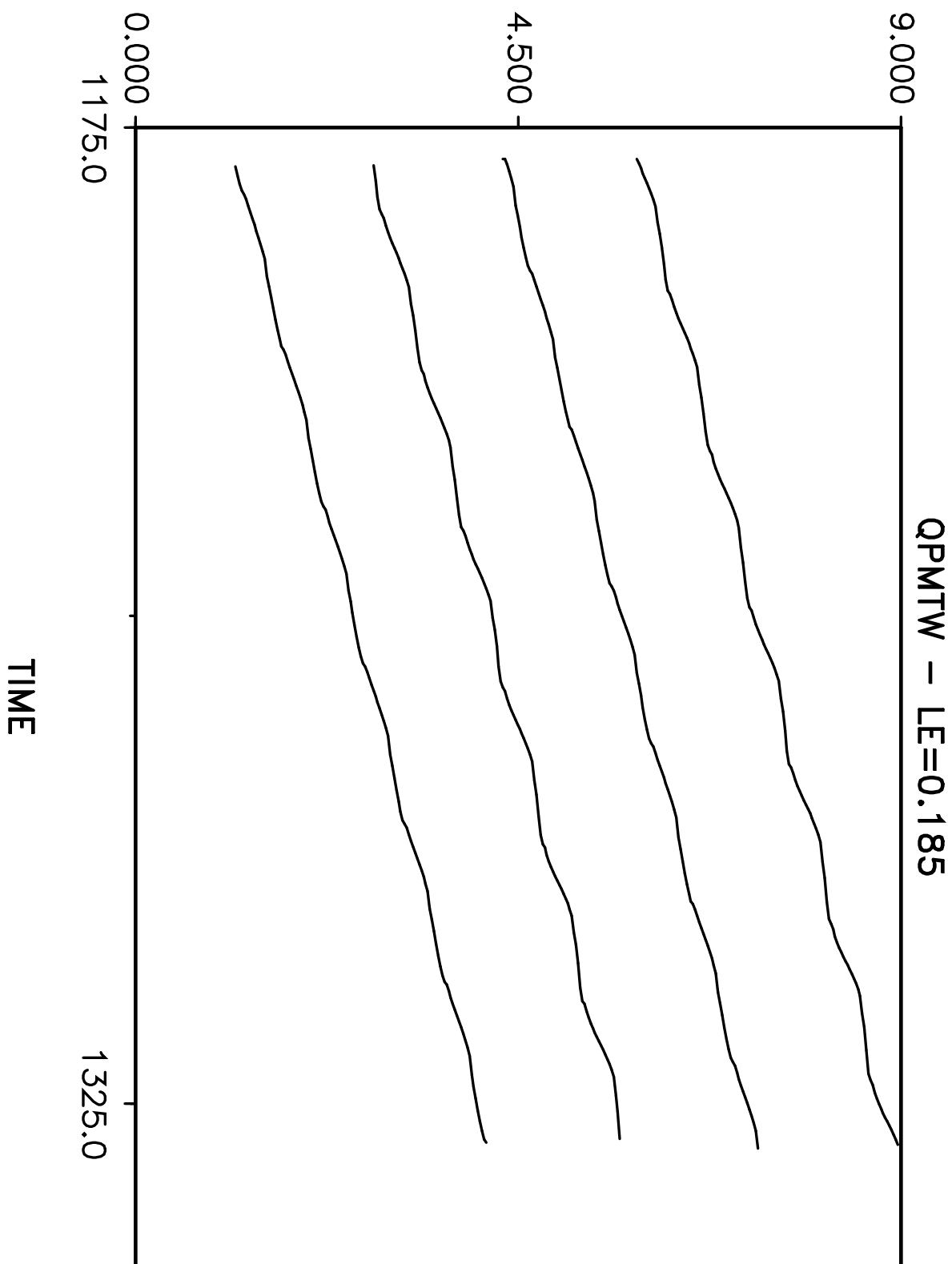


QPMTW - $L_e = 0.185$

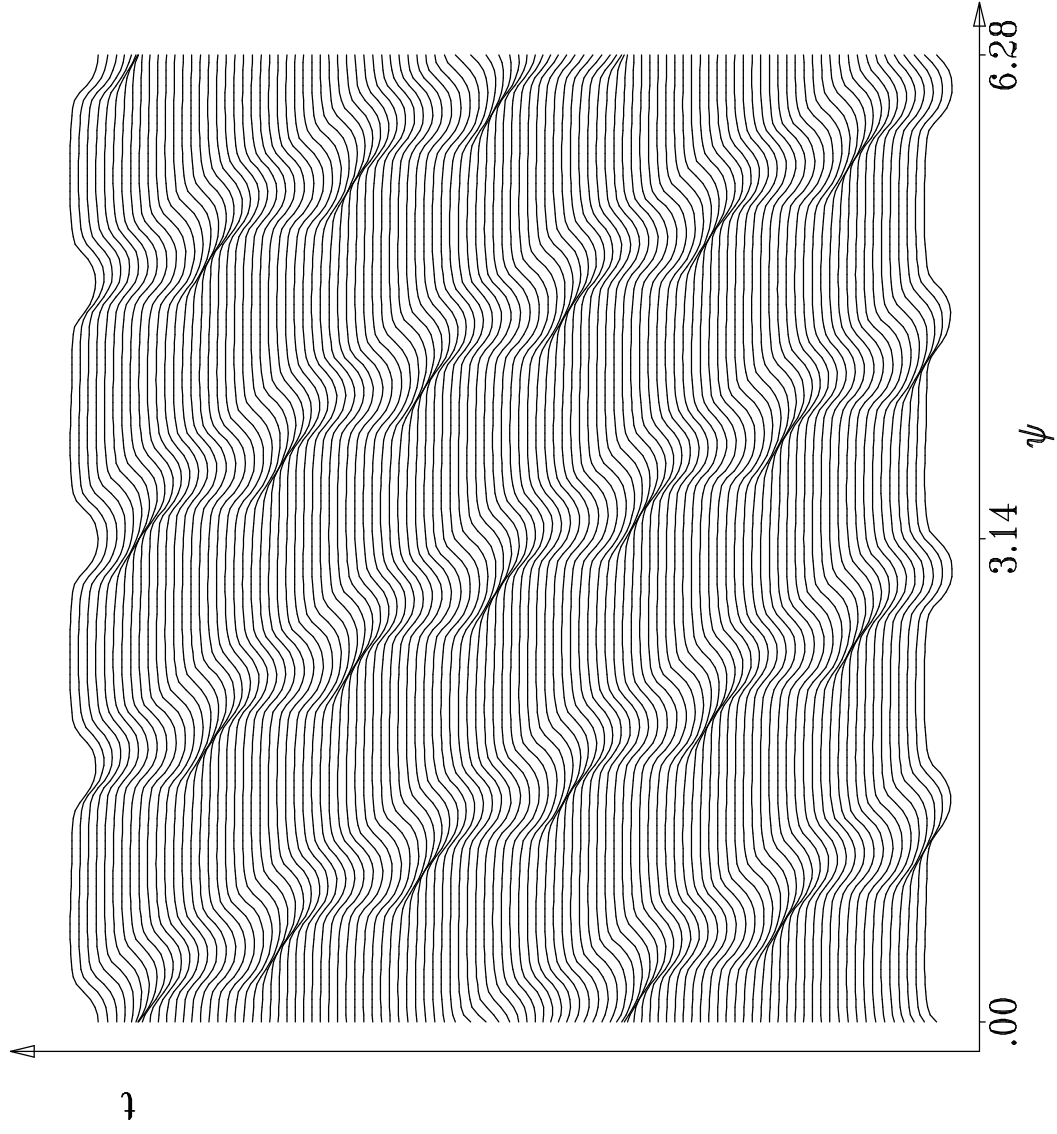


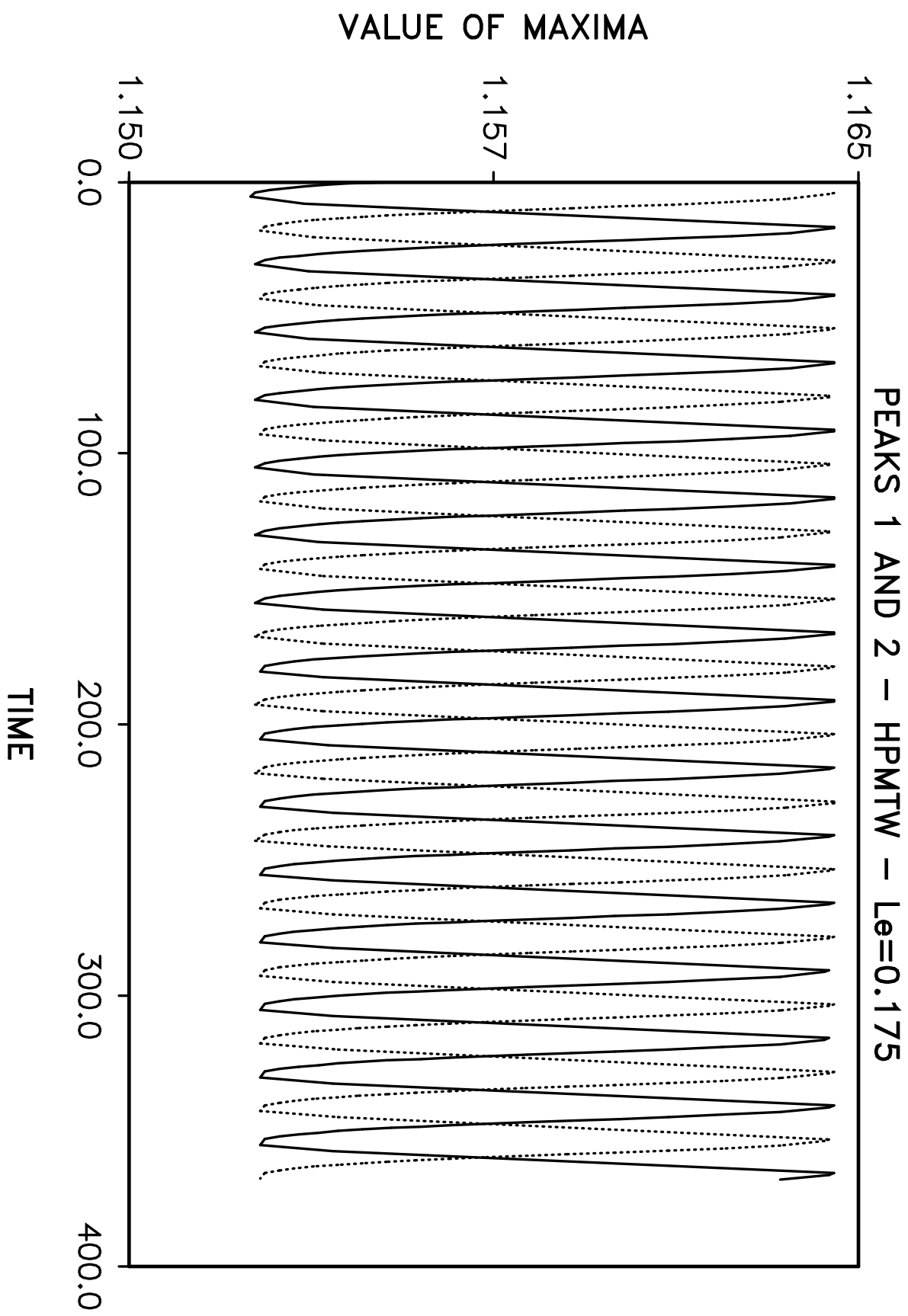
ω

ANGULAR LOCATION OF MAXIMA

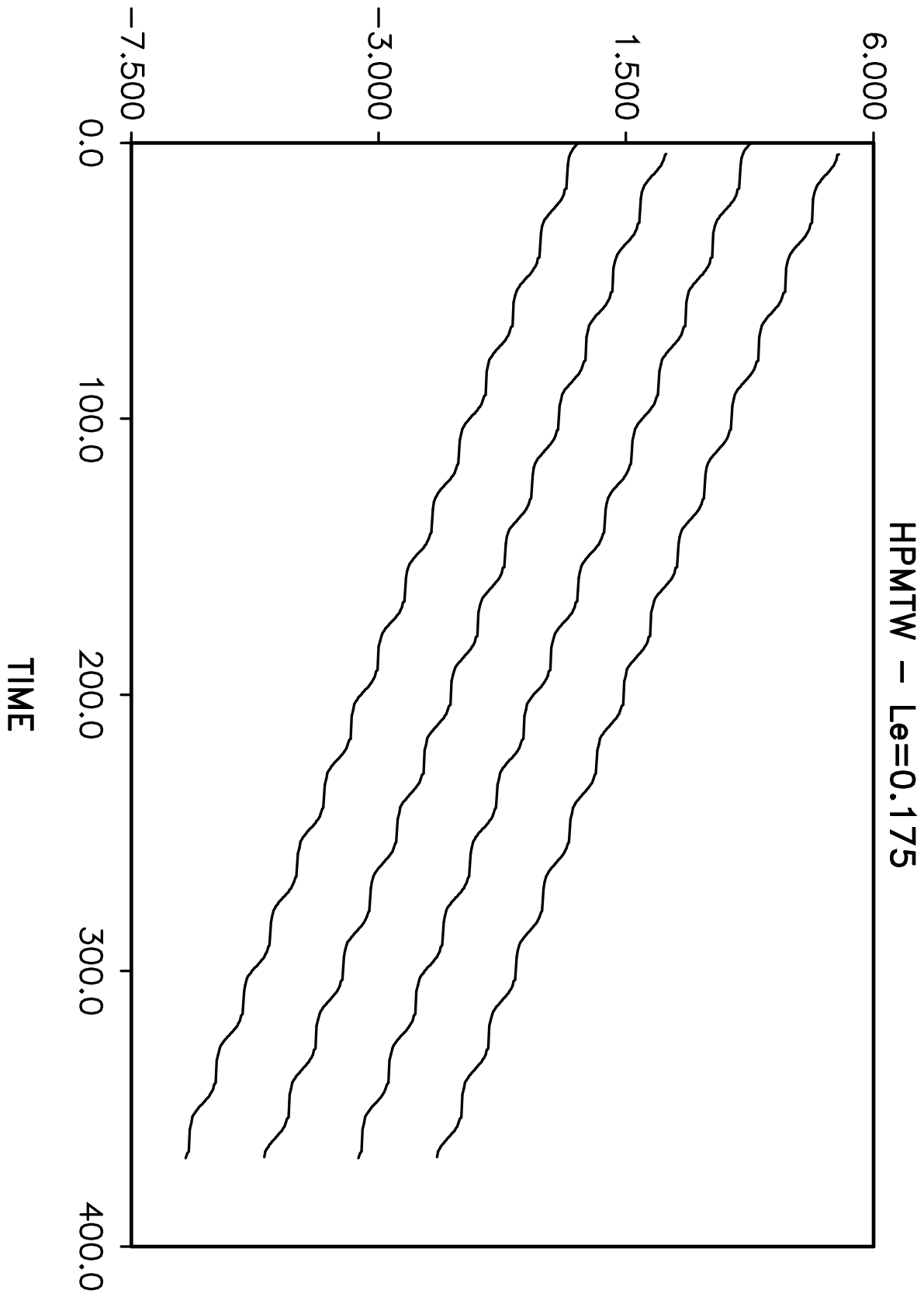


HPMTW BRANCH – $Le=0.175$

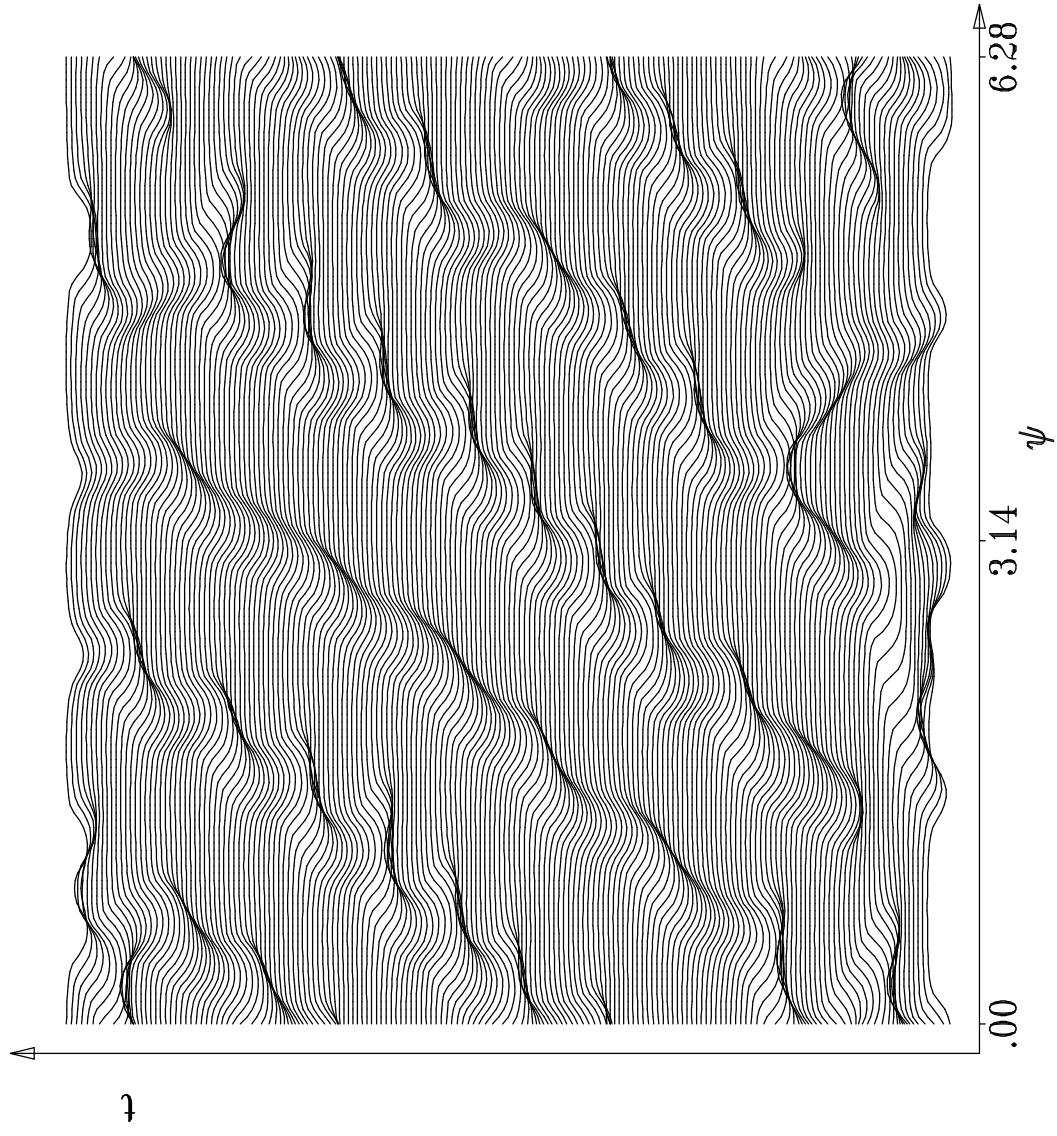




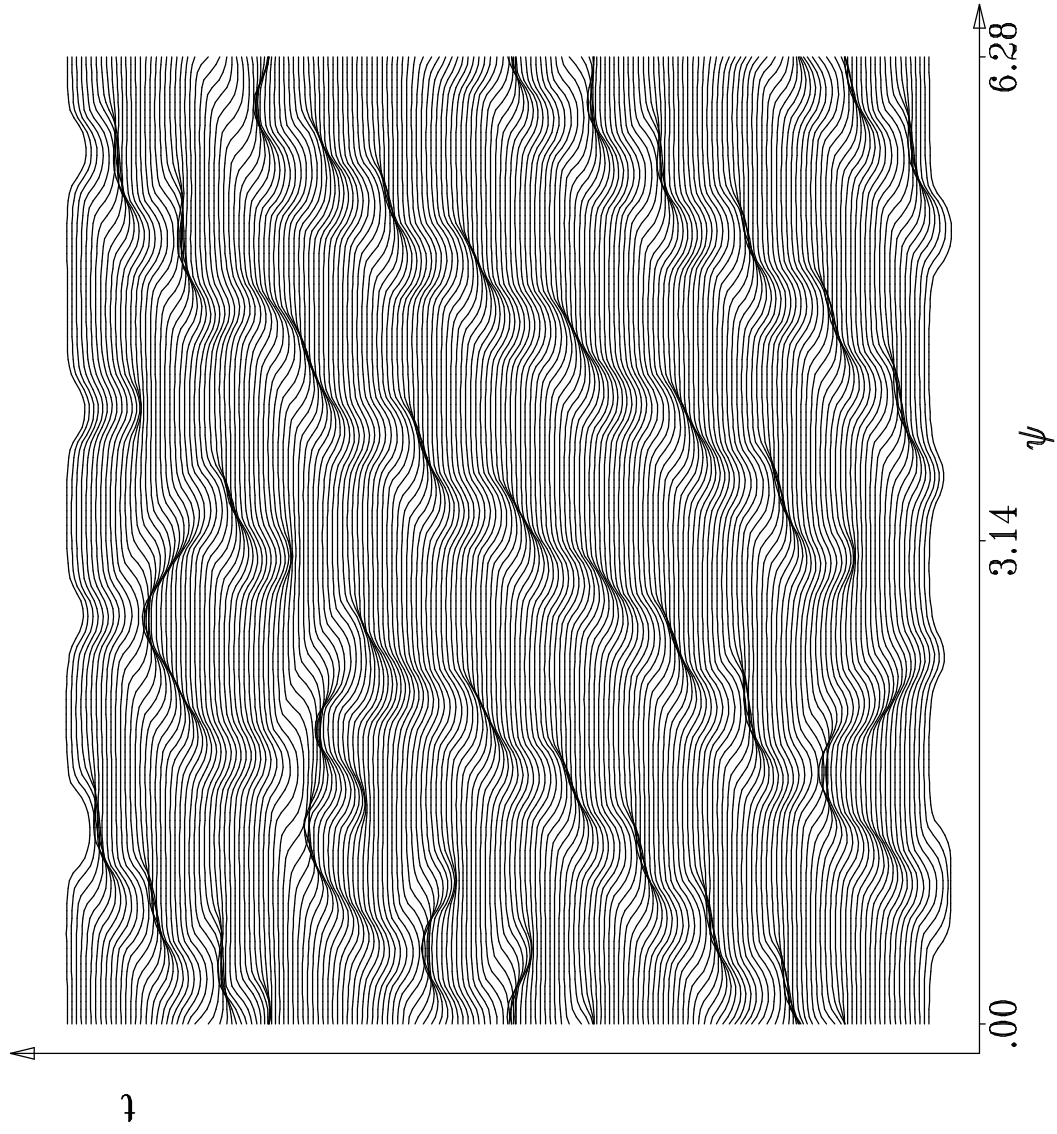
ANGULAR LOCATION OF MAXIMA

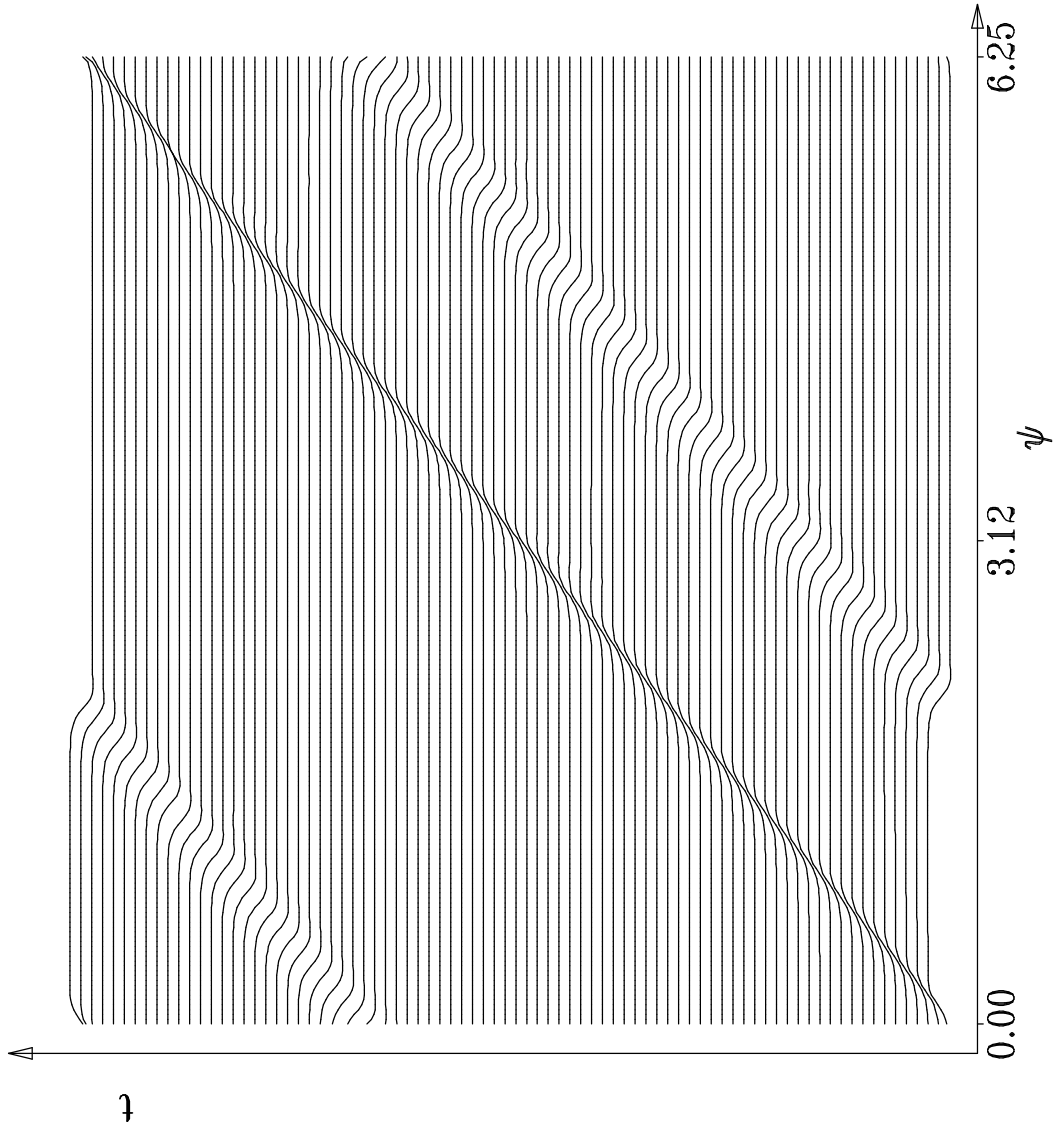


CHAOTIC BEHAVIOR – $Le=0.165$



CHAOTIC BEHAVIOR – $Le=0.165$





Stable Localized Wave for $b_2=0$

